

INTEGRATED STRATIGRAPHY OF THE MIDDLE–UPPER JURASSIC OF THE KRÍŽNA NAPPE, TATRA MOUNTAINS

Renata JACH¹, Nevenka DJERIĆ², Špela GORIČAN³ & Daniela REHÁKOVÁ⁴

¹ *Institute of Geological Sciences, Jagiellonian University, Oleandry 2a, 30-063 Kraków, Poland, e-mail: renata.jach@uj.edu.pl*

² *Faculty of Mining and Geology, Belgrade University, Djusina 7, Belgrade, Serbia, e-mail: djeranen@rgf.bg.ac.rs*

³ *Ivan Rakovec Institute of Palaeontology, ZRC SAZU, Novi trg 2, SI-1000 Ljubljana, Slovenia, e-mail: spela@zrc-sazu.si*

⁴ *Department of Geology and Palaeontology, Faculty of Natural Sciences, Comenius University, Mlynská dolina G-1, 842 15 Bratislava, Slovakia, e-mail: rehakova@fns.uniba.sk*

Jach, R., Djerić, N., Goričan, Š. & Reháková, D., 2014. Integrated stratigraphy of the Middle–Upper Jurassic of the Krížna Nappe, Tatra Mountains. *Annales Societatis Geologorum Poloniae*, 84: 1–33.

Abstract: Middle–Upper Jurassic pelagic carbonates and radiolarites were studied in the Krížna Nappe of the Tatra Mountains (Central Western Carpathians, southern Poland and northern Slovakia). A carbon isotope stratigraphy of these deposits was combined with biostratigraphy, based on radiolarians, calcareous dinoflagellates and calpionellids. In the High Tatra and Belianske Tatra Mountains, the Bajocian and part of the Bathonian are represented by a thick succession of spotted limestones and grey nodular limestones, while in the Western Tatra Mountains by relatively thin *Bositra*-crinoidal limestones. These deposits are referable to a deeper basin and a pelagic carbonate platform, respectively. The various carbonate facies are followed by deep-water biosiliceous facies, namely radiolarites and radiolarian-bearing limestones of Late Bathonian–early Late Kimmeridgian age. These facies pass into Upper Kimmeridgian–Lower Tithonian pelagic carbonates with abundant *Saccocoma* sp. The bulk-carbonate isotope composition of the carbonate-siliceous deposits shows positive and negative $\delta^{13}\text{C}$ excursions and shifts in the Early Bajocian, Late Bajocian, Early Bathonian, Late Bathonian, Late Callovian, Middle Oxfordian and Late Kimmeridgian. Additionally, the $\delta^{13}\text{C}$ curves studied show a pronounced increasing trend in the Callovian and a steadily decreasing trend in the Oxfordian–Early Tithonian. These correlate with the trends known from the Tethyan region. The onset of Late Bathonian radiolarite sedimentation is marked by a decreasing trend in $\delta^{13}\text{C}$. Increased $\delta^{13}\text{C}$ values in the Late Callovian, Middle Oxfordian and Late Kimmeridgian (Moluccana Zone) correspond with enhanced radiolarian production. A significant increase in CaCO_3 content is recorded just above the Late Callovian $\delta^{13}\text{C}$ excursion, which coincides with a transition from green to variegated radiolarites.

Key words: carbon and oxygen isotopes, radiolarians, calcareous dinoflagellates, radiolarites, Krížna Nappe, Western Carpathians, Tethys.

Manuscript received 11 November 2013, accepted 14 April 2014

INTRODUCTION

Radiolarites are one of the most typical facies of the Middle–Upper Jurassic successions in the Western Tethyan region. In the Alpine Tethys, the onset of biosiliceous sedimentation in various basins was diachronous and spanned from the earliest Bajocian to the Late Oxfordian (e.g., Bill *et al.*, 2001; Baumgartner, 2013). This kind of sedimentation continued until the Early Tithonian. Middle and Upper Jurassic radiolarites and associated deep-water carbonates were related to the breakup of Pangea and the opening of the Atlantic Ocean and the Alpine Tethys. Usually, the appearance of radiolarites was associated with sedimentation in basins with thinned continental crust, or in basins with oceanic crust (e.g., Bernoulli and Jenkyns, 1974; Bill *et al.*, 2001; Baumgartner, 2013 and references therein).

Previous studies from the Western Tethyan region have proved the value of carbon isotope ratios in the stratigraphic and palaeoenvironmental analysis of carbonate successions (e.g., Bartolini *et al.*, 1996; Jenkyns, 1996; Jenkyns *et al.*, 2002; Padden *et al.*, 2002; Weissert and Erba, 2004; Louis-Schmid *et al.*, 2007). Generally, pronounced positive $\delta^{13}\text{C}$ excursions in marine carbonates were caused by higher production of organic matter and its burial (e.g., Jarvis *et al.*, 2002; Colombié *et al.*, 2011). In contrast, major negative excursions are explained by the reworking and oxidation of organic matter. These isotope events usually coincided with long-term sea-level changes. In most cases, negative $\delta^{13}\text{C}$ events were associated with sea-level fall, positive ones with sea-level rise, whereas long-term declines in $\delta^{13}\text{C}$

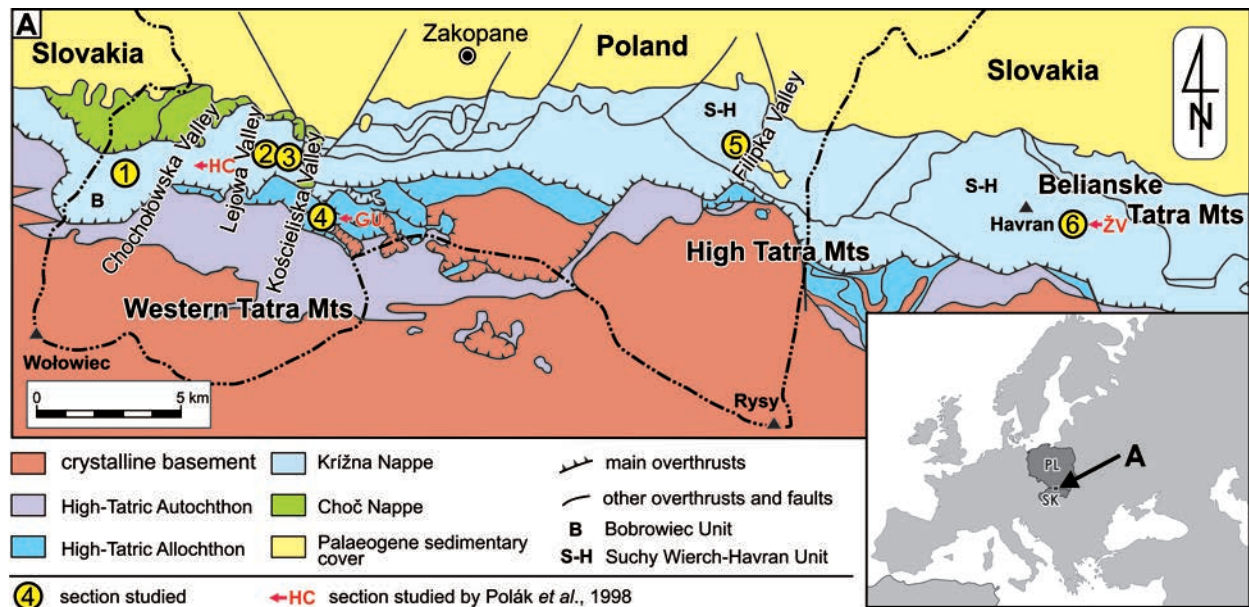


Fig. 1. Geological sketch map of the Tatra Mountains (after Bac-Moszaszwili *et al.* 1979; Nemčok *et al.*, 1994, simplified) showing location of the sections studied, (1) Długa Valley, (2) Lejowa Valley, (3) Zadnia Kopka Kościeliska, (4) Upląziańska Kopa, (5) Filipka Valley and (6) Ždiarska Vidla (Płaczliwa Skała in Polish); sections studied by Polák *et al.* (1998), (HC) Banie Huciska, (GU) Gładkie Upląziańskie (=Upląziańska Kopa) and (ŽV) Ždiarska Vidla.

trends after transgression are linked to increased carbonate precipitation and accumulation (e.g., Jarvis *et al.*, 2002). It is noteworthy that high biosiliceous productivity associated with a crisis in carbonate production appears to be correlated with positive $\delta^{13}\text{C}$ events (e.g., Bartolini *et al.*, 1996; Racki and Cordey, 2000; Morettini *et al.*, 2002; O'Dogherty *et al.*, 2006).

Tethyan successions containing radiolarites have been studied widely, in terms of depositional processes, bio- and chemostratigraphy as well as their significance to the record of climate changes (Baumgartner, 2013 and references therein). Correlation of regional biostratigraphic schemes often remains ambiguous, because of the mosaic facies pattern characteristic for the Middle Jurassic and diverse biostratigraphic tools (e.g., ammonites, calcareous nannofossils and radiolarians), which are applied in various deposits. In such cases, stable isotope stratigraphy appears to be a useful method for correlation, both at the regional and global scales. It is a useful tool for chemostratigraphy, since the Middle–Late Jurassic $\delta^{13}\text{C}$ curve is characterized by well-recognized isotopic events, which are calibrated against biostratigraphic data (e.g., Bartolini *et al.*, 1999; O'Dogherty *et al.*, 2006; Louis-Schmid *et al.*, 2007).

This study focuses on a peculiar sedimentary succession of Middle–Late Jurassic age, exposed in the Tatra Mountains (Central Western Carpathians). This succession, belonging to the Križna Nappe, is characterized by a typical Tethyan basinal development with dominance of carbonate-biosiliceous sedimentation (Lefeld, 1974; Lefeld *et al.*, 1985). The sections studied are described on the basis of lithology, biostratigraphic data (radiolarians, calcareous dinoflagellates and calpionellids) and the carbon isotope record, which is compared mainly to the reference $\delta^{13}\text{C}$ curves from the Tethyan and peri-Tethyan regions.

The objectives of this paper are: (1) to document the facies succession of the radiolarian-bearing deposits of the Križna Nappe in the Tatra Mountains, (2) to propose a biostratigraphic framework for the radiolarian and calcareous dinoflagellate zone levels, (3) to generate $\delta^{13}\text{C}$ isotope curves calibrated against biostratigraphic data, (4) to correlate $\delta^{13}\text{C}$ curves from the sections studied and (5) to compare them with the reference curves.

GEOLOGICAL SETTING

The Middle–Upper Jurassic deposits of the Križna Nappe examined crop out in the Tatra Mountains (Central Western Carpathians) in Poland and Slovakia (Fig. 1; Bac-Moszaszwili *et al.*, 1979; Nemčok *et al.*, 1994). The Križna Nappe represents one of the sedimentary nappes overlying the crystalline core of the Tatra Mountains (Lefeld *et al.*, 1985). It comprises Lower Triassic to Lower Cretaceous deposits and is made up of several thrust slices.

The Križna Nappe belongs to the Faticum Domain in the Central Carpathian block (Plašienka, 2012). During most of Jurassic time, it was one of the domains lying between the Alpine Tethys to the north and the Meliata Ocean to the south (Fig. 2; Csontos and Vörös, 2004; Schmid *et al.*, 2008). As a consequence of its location, the succession studied shows a strong similarity to the Jurassic of other Tethyan basins.

During the Jurassic, the Faticum Domain was bordered by the uplifted Tatricum Domain to the north and the Veporicum Domain to the south. The Faticum Domain was regarded as being an extensional basin during the Jurassic, located on thinned and stretched continental crust (e.g., Plašienka, 2012). As a result, the Jurassic successions of the

Fatricum Domain are characterized by an almost continuous record of the prograding Tethyan transgression, displaying a transition from littoral through hemipelagic to pelagic deep-sea sedimentation.

The Jurassic deposits of the Krížna Nappe in the Tatra Mountains represent deep-water successions of the Zliechov type (Maheľ and Buday, 1968; Michalík, 2007). The Early Jurassic phase of extension gave rise to wide basinal areas and narrow horsts (Plašienka, 2012). A second phase of extension took place during the latest Early Jurassic and resulted in the extensional tilting of blocks, forming a horst-and-graben topography (Wieczorek, 1990; Gradziński *et al.*, 2004; Jach, 2005; Plašienka, 2012). The formation of horsts (Bobrowiec Unit and the Gładkie Uplaziańskie Thrust Slice in the Western Tatra Mountains) and grabens (the Suchy Wierch–Havran Unit in the High Tatra and Belianske Tatra Mountains) led to distinct facies changes (Guzik, 1959; Jach, 2007). The subsiding basins constantly were filled with Fleckenmergel-type sediments (bioturbated “spotted” limestones and marls, ranging from the Sinemurian to the Bajocian). The horsts during the Late Pliensbachian–?Aalenian acted as submarine highs with spiculite (Jach, 2002) and neritic crinoidal sedimentation (e.g., crinoidal tempestites; Jach, 2005), replaced by condensed pelagic carbonates that were deposited on pelagic carbonate platforms (*sensu* Santantonio, 1993). During the Middle Jurassic, significant topographic relief was still present and controlled facies changes. The deposition of carbonate sediments terminated with the onset of uniform radiolarite sedimentation during the late Middle Jurassic. The complete recovery of carbonate sedimentation took place during the latest Jurassic.

A formal lithostratigraphy of the Middle–Upper Jurassic deposits in the Tatra Mountains was proposed by Lefeld *et al.* (1985). In the interval studied, the following units were distinguished: the Sołtysia Marlstone Formation, comprising the Łomy Limestone Member (spotted limestones with marls) and the Broniarski Limestone Member (cherty limestones); the Niedzica Limestone Formation (grey nodular limestones); the Sokolica Radiolarite Formation (spotted and green radiolarites); the Czajakowa Radiolarite Formation (variegated and red radiolarites); the Czorsztyń Limestone Formation (red nodular limestones); and the Pieniny Limestone Formation (platy limestones). The last mentioned limestones were assigned to a new formal unit, the Jasenina Formation (Michalík *et al.*, 1990; Grabowski and Pszczółkowski, 2006).

Polák *et al.* (1998) redefined the previously recognized Sokolica Radiolarite Formation and Czajakowa Radiolarite Formation and proposed the Ždiar Formation as a new unit, comprising the entire radiolarite succession. In this study, the formal lithostratigraphy by Lefeld *et al.* (1985) is used, with the exception of the Jasenina Formation.

PREVIOUS RESEARCH

A few attempts have been made to determine the age of the radiolarites of the Krížna Nappe in the Tatra Mountains. Rabowski and Goetel (1925) estimated their age as Middle Jurassic, whereas Sujkowski (1932) suggested Middle–Late Jurassic, on the basis of their position in the succession.

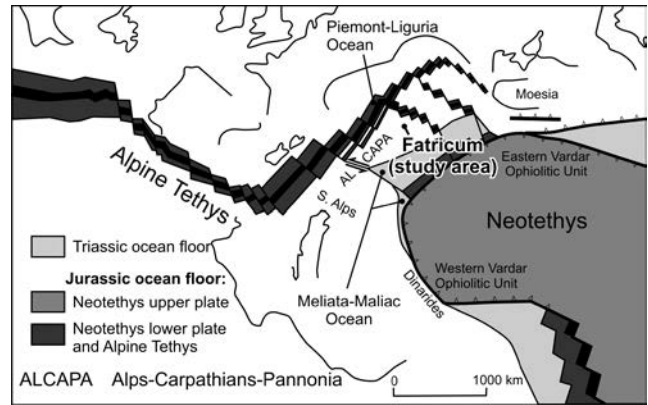


Fig. 2. Palaeogeographic position of the Fatricum Domain in the Oxfordian. After Schmid *et al.* (2008), simplified.

The first biostratigraphic data have come from the aptychi, collected in the Grześ section in the Western Tatra Mountains (Gašiorowski, 1959, 1962). They give the age of the red radiolarites and red nodular limestones as Late Oxfordian–Early Tithonian; hence the underlying radiolarites were regarded as Middle Jurassic–Oxfordian. Detailed descriptions of the Middle–Upper Jurassic successions of the Krížna Nappe, comprising radiolarites, were presented by Lefeld (1969, 1974, 1981). The ammonite stratigraphy of the Early and Middle Jurassic was provided by Myczyński and Lefeld (2003), Myczyński (2004), Myczyński and Jach (2009) and later elaborated by Iwańczuk *et al.* (2013).

The age of the Tatra radiolarites was estimated on the basis of radiolarians to be Late Bathonian–Early Kimmeridgian (Polák *et al.*, 1998) or Middle Bathonian for the lowermost part of the Sokolica Radiolarite Formation (Bąk, 2001). More precise dating refers to the Late Kimmeridgian and Early Tithonian, where calcareous dinoflagellates permit the recognition of discrete zones, starting from the Late Kimmeridgian calcareous dinoflagellate *Moluccana* Zone in the upper part of red radiolarites (Jach *et al.*, 2012). Higher stratigraphic resolution was achieved in the uppermost Lower Tithonian Jasenina Formation, where chitinoideids and calpionellids (Lefeld, 1974; Pszczółkowski, 1996), combined with magnetostratigraphy (Grabowski and Pszczółkowski, 2006), permitted the establishment of a precise stratigraphic scheme (Grabowski *et al.*, 2013).

METHODS

The sections (Table 1; Figs 3–8) were analysed at high resolution, including microfacies analysis, carbonate content, biostratigraphy, and analysis of carbon and oxygen isotopes. Microfacies as well as the cysts of calcareous dinoflagellates were studied in 240 thin sections under Carl Zeiss Axioskop and LEICA DM 2500P optical microscopes. Dunham’s (1962) classification of microfacies was applied to the carbonate and siliceous sediments. The calcareous dinoflagellate zonations, proposed by Borza (1984) and Borza and Michalík (1986), later revised by Reháková (2000), and the

Table 1

Location of the sections studied

Section name	Code	Location	Coordinates at base of section	Tectonic unit
Długa Valley	Dsp, Dsr	Western Tatra Mts, Poland	N49°15.599'; E19°48.014'	Bobrowiec Unit
Lejowa Valley	L		N49°15.913'; E19°50.883'	
	Lb		N49°15.905'; E19°50.933'	
	Lc		N49°15.897'; E19°50.979'	
	Ld		N49°15.960'; E19°50.879'	
Zadnia Kopka Kościeliska	Pk		N49°15.570'; E19°51.848'	
Uplazińska Kopa	Gd		N49°14.359'; E19°53.275'	Gładkie Uplazińskie Thrust Slice
Filipka Valley	Fp	High Tatra Mts, Poland	N49°15.952'; E20°4.325'	Suchy Wierch-Havran Unit
	Fz		N49°16.137'; E20°4.348'	
<td>Fk</td> <td></td> <td></td> <td></td>	Fk			
Ždiarska Vidla	P	Belianske Tatra Mts, Slovakia	N49°14.588'; E20°12.636'	

calpionellid biostratigraphic scheme, proposed by Reháková (2002), were adopted. The rock samples and the thin sections are stored at the Institute of Geological Sciences, Jagiellonian University in Kraków.

For the radiolarian analyses, 61 samples were collected from different lithologies, but only 16 samples with poor to moderately preserved radiolarians were selected for detailed biostratigraphic studies (locations in Figs 3–8). The radiolarian-bearing samples were etched with hydrochloric and hydrofluoric acid, utilizing standard methods (Pessagno and Newport, 1972). The observations under the SEM for the precise identification and illustration of the radiolarians were performed at the University of Belgrade, in the SEM-EDS Laboratory of Faculty of Mining and Geology, using a JEOL JSM-6610LV microscope. In this paper, the radiolarian zonation based on the Unitary Association Zones (UAZs), proposed by Baumgartner *et al.* (1995), was adopted. The names of genera were corrected with reference to the new revision by O'Dogherty *et al.* (2009).

The stable isotope compositions of carbon and oxygen were studied in 367 bulk sediment samples. Sections were sampled at approximately 0.5–1 m intervals, exceptionally at more than 2 m. Both limestones and radiolarites containing a carbonate fraction were analysed. Only homogenous micritic samples were selected. In each case, the sample weight was adjusted according to the CaCO₃ content. Carbon and oxygen stable isotope compositions ($\delta^{13}\text{C}$ and $\delta^{18}\text{O}$) were analysed in the Warsaw Isotope Laboratory for Dating and Environment Studies at the Institute of Geological Sciences, Polish Academy of Sciences. To produce the rockpowder samples, a diamond-tipped drill was used. The powder was reacted with 100% phosphoric acid (density 1.94 g/cm³) at 70°C, using the Kiel IV online carbonate preparation device, connected to the Thermo-Finnigan Delta+ mass spectrometer. The quality of analysis was controlled by measurements of the international standard NBS-19 with any sample series (3–5 NBS-19 measurements per samples series). All values are reported in per mil relative to V-PDB. Reproducibility was checked on the basis of long-term repeatability of NBS19 analysis and occurred better than 0.07 and 0.12‰, for $\delta^{13}\text{C}$ and $\delta^{18}\text{O}$, respectively.

The calcium carbonate content of 376 rock samples was estimated by means of a calcimetre by Eijkelkamp, which works in accordance with the method of Scheibler. The analysis of CaCO₃ content was conducted at the Institute of Geological Sciences of the Jagiellonian University in Kraków.

FACIES

On the basis of lithology, rock colour, fabric and carbonate content, nine facies were distinguished within the sections studied. They are as follows: (1) spotted limestones, (2) grey nodular limestones, (3) *Bositra*-crinoidal limestones, (4) spotted radiolarites, (5) green radiolarites, (6) variegated radiolarites, (7) red radiolarites, (8) red nodular limestones, and (9) platy limestones. In this paper, the term *Bositra* denotes thin-shelled bivalves (filaments), most probably belonging to the genus *Bositra*.

Spotted limestones

The spotted limestones (facies equivalent of the Allgäu Formation or “Fleckenmergel” in the Eastern Alps) make up the topmost part of the Sołtysia Marlstone Formation (Lefeld *et al.*, 1985). It is divided into two members – the lower Łomy Limestone Member, composed of spotted limestones and marls, and the upper Broniarski Limestone Member, with cherty limestones. These deposits are known from the High Tatra (Tatry Wysokie in Polish) and Belianske Tatra (Tatry Bielskie in Polish) Mountains.

The spotted limestones and marls (the measured thickness is 60 m) are represented by grey, bedded limestone-marl succession (Ždiarska Vidla section; Fig. 8). The limestones form 3–60 cm thick beds, whereas the marls are approximately 10 cm, maximally 90 cm thick. Abundant trace fossils are preserved as dark spots, visible against a totally bioturbated light grey background. The limestone beds display symmetrical silicification of their lower and upper parts. Seven beds of grey crinoidal turbidites, 8–46 cm thick, occur in the Ždiarska Vidla section, in the lower- and uppermost parts of the facies (at the 1 m, 5.3 m, 6.5 m, 48 m,

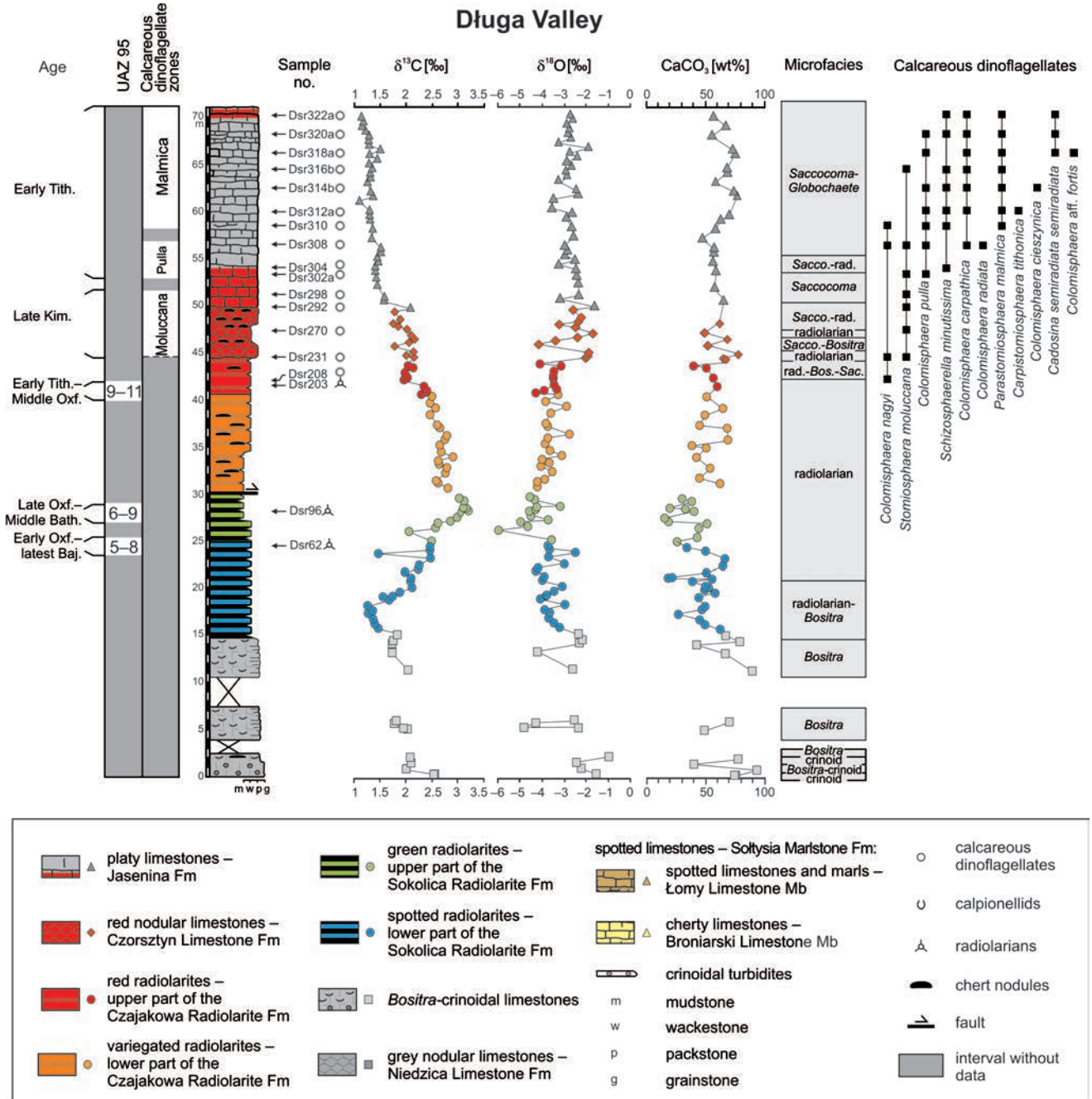


Fig. 3. Długa Valley section in the Western Tatra Mountains. Lithology, biostratigraphy (including position of the radiolarian and calcareous dinoflagellate samples) and results for carbon and oxygen isotope measurements, CaCO_3 content and microfacies analysis. Age denotes calibration of radiolarian (UAZ 95) or calcareous dinoflagellata zones. Legend for lithologies in Figs 3–8.

48.3 m, 50 m, 57 m; Fig. 8; see also Mišik, 1959). The CaCO_3 content fluctuates from 6 to 91 wt%; the average value is about 54 wt% (Fig. 8).

In the spotted limestones and marls, six microfacies types were distinguished (Fig. 8): spiculite-Bositra packstone, spiculite wackestone, Bositra packstone, crinoid wackestone and grainstone, and crinoid-spiculite wackestone. Beside coarse-grained crinoidal material, quartz and other lithic grains are common. Ammonites occur rarely in the spotted limestones and marls.

The upper part of the spotted limestones is represented

by cherty limestones, about 23 m thick (Figs 7, 8). The transition to the overlying grey nodular limestones (Niedzica Limestone Formation) is gradual. Dark brownish-grey cherty limestones are thin- to medium-bedded, rarely intercalated with marls. Trace fossils become less common upwards in the section. In the topmost part, elongated, dark grey chert nodules are abundant. In the Filipka Valley, the uppermost part of the cherty limestones consists of cherty radiolarian limestones (Fig. 7). Generally, the CaCO_3 content is relatively low, ranging from 30 to 68 wt% (Figs 7, 8).

The following microfacies were distinguished in the

The light grey nodular limestones are medium- to thick-bedded and locally indistinctly bedded. They are pale pink only in the uppermost part of the Filipka Valley section. Carbonate nodules occur in various sizes and are separated by thin bands of dissolution seams, rich in clays, muscovite and silty quartz. Irregular chert nodules form distinct horizons. A massive graded breccia bed, 70 cm thick, is found within the grey nodular limestones of the Filipka Valley section (42 m; Fig. 7). It is composed of crinoid material, with angular clasts (up to 2 cm) of spiculites, crinoidal limestones and other sedimentary rocks. The average CaCO_3 content is about 57 wt%, with a range of 33 to 82 wt% (Figs 7, 8).

Thin sections of grey nodular limestones show the following microfacies (Figs 7, 8): crinoid wackestone, *Bositra*-spiculite, *Bositra* and *Bositra*-crinoid wackestone to packstone, and *Bositra*-radiolarian wackestone. Belemnite rostra and poorly preserved moulds of ammonites are found rarely.

Bositra-crinoidal limestones

Limestones with *Bositra* and crinoids (up to 15.5 m thick) do not have any formal lithostratigraphic status. This facies occurs only in the Western Tatra Mountains (Tatry Zachodnie in Polish). The base of the *Bositra*-crinoidal limestones is marked by an omission surface (Gradziński *et al.*, 2004; Jach, 2007) at the top of the Toarcian–?Aalenian red nodular limestones (Kliny Limestones Member). The transition to the overlying spotted radiolarites is marked by a decrease in CaCO_3 content (Figs 3, 4).

The lowermost part of the *Bositra*-crinoidal limestones is composed of pinkish to grey crinoidal turbidites, with beds up to 20 cm thick, intercalated with glauconitic marls (Jach, 2007). The total thickness of this part is 1.7 m in the Długa Valley section and 0.3 m in the Lejowa Valley section (Figs 3, 4). The glauconitic marls exhibit some of the characteristics of condensed deposits. Towards the top of the *Bositra*-crinoidal limestones, crinoidal intercalations become less common and disarticulated *Bositra* shells begin to predominate, leading to formation of the *Bositra* limestones (3.3–14 m thick; Figs 3, 4). They are grey, greenish-grey, well bedded, locally with elongated dark grey chert nodules. The average CaCO_3 content of the *Bositra*-crinoidal limestones is about 68 wt%, ranging from 36 up to 93 wt% (Figs 3, 4).

In thin sections, the *Bositra*-crinoidal limestones show a succession of the following microfacies (Figs 3, 4): crinoid packstone-grainstone, *Bositra* packstone-grainstone, *Bositra*-crinoid packstone, and *Bositra*-radiolarian wackestone.

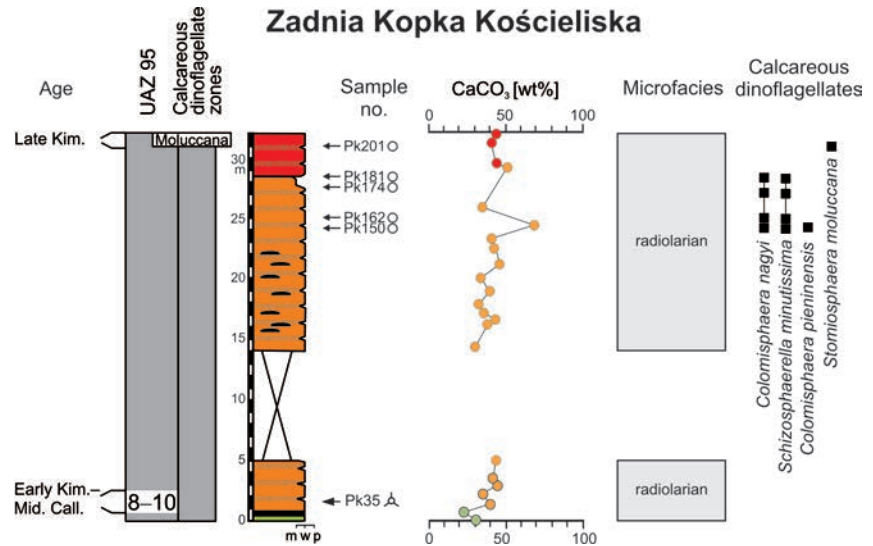


Fig. 5. Zadnia Kopka Kościeliska section in the Western Tatra Mountains. Lithology, biostratigraphy (including position of the radiolarian and calcareous dinoflagellate samples) and CaCO_3 content and microfacies analysis. Age denotes calibration of radiolarian (UAZ 95) or calcareous dinoflagellata zones. Legend for lithologies as in Fig. 3.

Spotted radiolarites

The spotted radiolarites (9–15 m thick), also comprising radiolarian limestones, belong to the lower part of the Sokolica Radiolarite Formation (Lefeld *et al.*, 1985). They are present in all of the sections studied (Figs 3–5, 7, 8), with the exception of the Zadnia Kopka Kościeliska and Uplaziańska Kopa sections. The contact with the overlying green radiolarites is sharp in the Długa Valley section, but is gradual in the Filipka Valley and Ždiarska Vidla sections (Figs 3–5, 7, 8).

Radiolarites and radiolarian limestones are grey and towards the top olive-grey, with common shale intercalations 1–3 cm thick. They are distinctly bedded, with beds about 10–15 cm thick. Abundant trace fossils are observed as dark spots, visible against the lighter bioturbated background. Elongated dark grey chert nodules are common in the middle parts of beds in the Filipka Valley and Ždiarska Vidla sections. A subtle lamination is visible under the microscope in the uppermost part of this facies. The average CaCO_3 content is about 36 wt%, ranging from 12 up to 69 wt% (Figs 3–5, 7, 8).

Four microfacies were distinguished in the spotted radiolarites (Figs 3–5, 7, 8): radiolarian-*Bositra* wackestone, *Bositra* wackestone, radiolarian wackestone to packstone and mudstone. They also contain sponge spicules, crinoid ossicles, the tests of ostracods and fragments of the tests of foraminifera. Locally, the matrix contains silty clastic grains (muscovite and quartz).

Green radiolarites

The green radiolarites (up to 12 m thick) were assigned to the upper part of the Sokolica Radiolarite Formation (Figs 3–8; Lefeld *et al.*, 1985). They are present in all of the

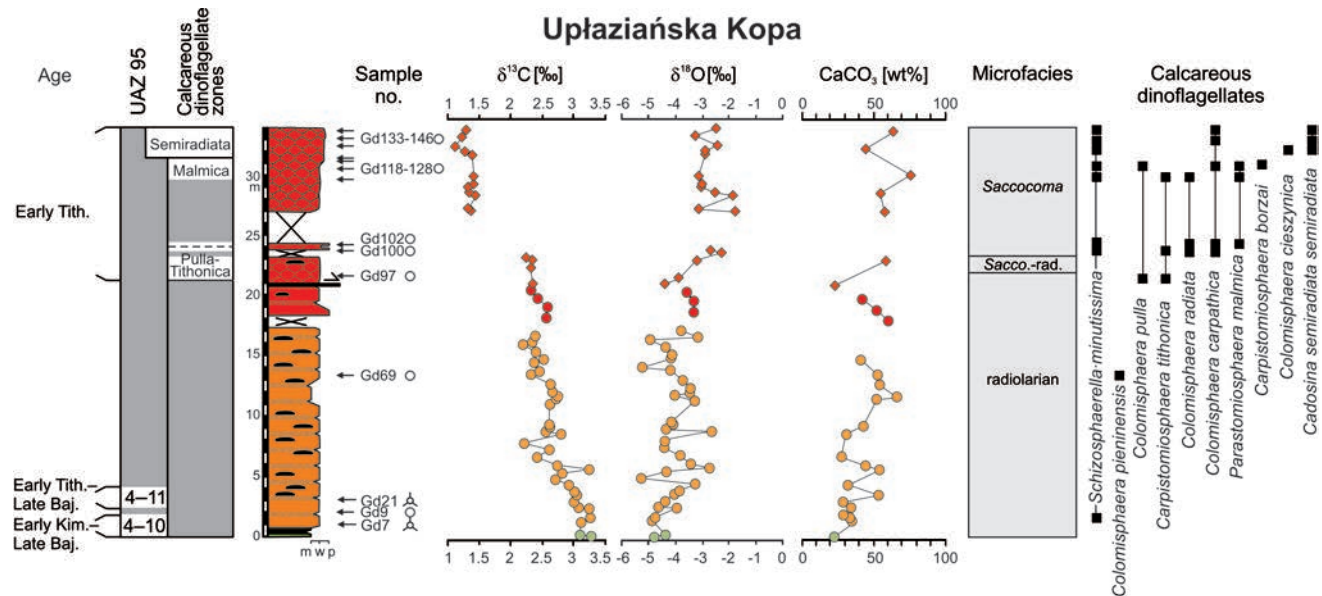


Fig. 6. Uplazińska Kopa section in the Western Tatra Mountains. Lithology, biostratigraphy (including position of the radiolarian and calcareous dinoflagellate samples) and results for carbon and oxygen isotope measurements, CaCO_3 content and microfacies analysis. Age denotes calibration of radiolarian (UAZ 95) or calcareous dinoflagellata zones. Legend for lithologies as in Fig. 3.

sections studied (Figs 3–8). An abrupt transition from the green radiolarites to the overlying variegated radiolarites is accompanied by an increase in CaCO_3 content.

Highly siliceous radiolarites are mostly green, greenish grey and light olive grey. Only in the eastern part of the Tatra Mountains, they are dark grey and dark olive grey. Thin- to medium-bedded, ribbon radiolarites alternate with siliceous shales, 0.2–2 cm thick. These chert-shale couplets are the most characteristic feature of the green radiolarites. Some beds display centimetre-thick partitioning, more or less parallel to the bedding. The average CaCO_3 content is about 25 wt%, ranging from 7 up to 48 wt% (Figs 3, 4, 6–8).

In thin sections, the green and grey radiolarites are characterized by radiolarian mudstone-wackestone microfacies, with calcified and extensively dissolved radiolarian tests, very rare *Bositra* and fragments of the tests of foraminifera (Figs 3–8). At a microscopic scale, a subtle lamination is relatively common and reflects changes in radiolarian content. Cryptocrystalline silica occurs mainly in the matrix.

Variegated radiolarites

The variegated radiolarites, identified in all of the sections studied, correspond to the lower part of the Czajakowa Radiolarite Formation (Figs 3–8; Lefeld *et al.*, 1985). The transition to the overlying red radiolarites is gradual. Measured thicknesses vary from 5 to 17 m.

In the Western Tatra Mountains, the variegated radiolarites are calcareous, and distinctly bedded, with bed thicknesses of about 10–15 cm. They are characterized by a noticeably higher average content of CaCO_3 , the common occurrence of chert nodules and the very rare occurrence of thin shale intercalations. They exhibit a variety of colours; in the lower part, they are light olive, dusky red, and pale

green to yellowish grey, while towards the top, they are pale red, pale olive, olive grey, red and red-green. Intensely reddish or greyish massive chert nodules are typical of this facies, especially in the Uplazińska Kopa section. The average CaCO_3 content is about 50 wt% (Figs 3–8).

In the High Tatra and Belianske Tatra Mountains, variegated radiolarites are pale reddish brown, with grey or light brown spots of diffusive type and with dark grey chert nodules. Shale intercalations are absent. The CaCO_3 average content is about 44 wt%, ranging from 24 up to 67 wt% (Figs 3–8).

In thin sections, the variegated radiolarites show an upward transition from radiolarian mudstone to packstone (Figs 3–8). They contain radiolarians, sponge spicules, crinoids, planktonic foraminifer *Globuligerina* and cysts of calcareous dinoflagellates. Radiolarians are calcified or partially silicified.

Red radiolarites

The uppermost part of the Czajakowa Radiolarite Formation consists of red radiolarites, exposed in all of the sections studied (Figs 3–8; Lefeld *et al.*, 1985). Their thickness ranges from 2 to 9 m. The red radiolarites are calcareous, moderate red and greyish red in colour, and planar, thin- to medium-bedded, with bed thicknesses of between 5 and 30 cm. The red radiolarites are characterized by the rare occurrence of thin shale intercalations. In the Ždiarska Vidla section, the red radiolarites are cherty and irregularly bedded. Their average CaCO_3 content is about 48 wt%, ranging from 17 up to 89 wt% (Figs 3–8).

The red radiolarites contain indistinctly laminated radiolarian wackestone, locally passing into mudstone, radiolarian-*Bositra*-*Saccocoma* wackestone, *Saccocoma*-*Bositra* wackestone, *Bositra*-*Saccocoma* wackestone and radiola-

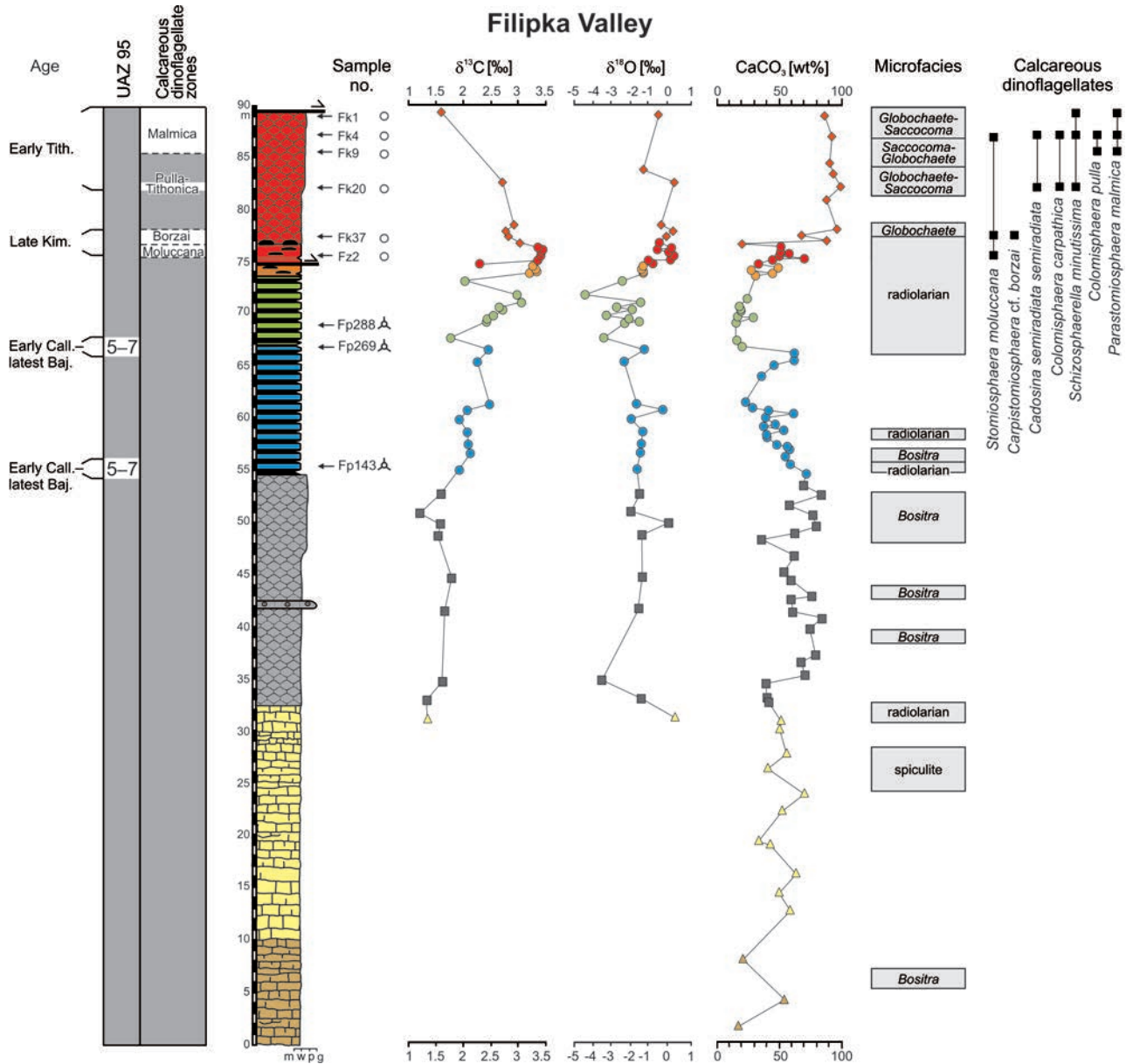


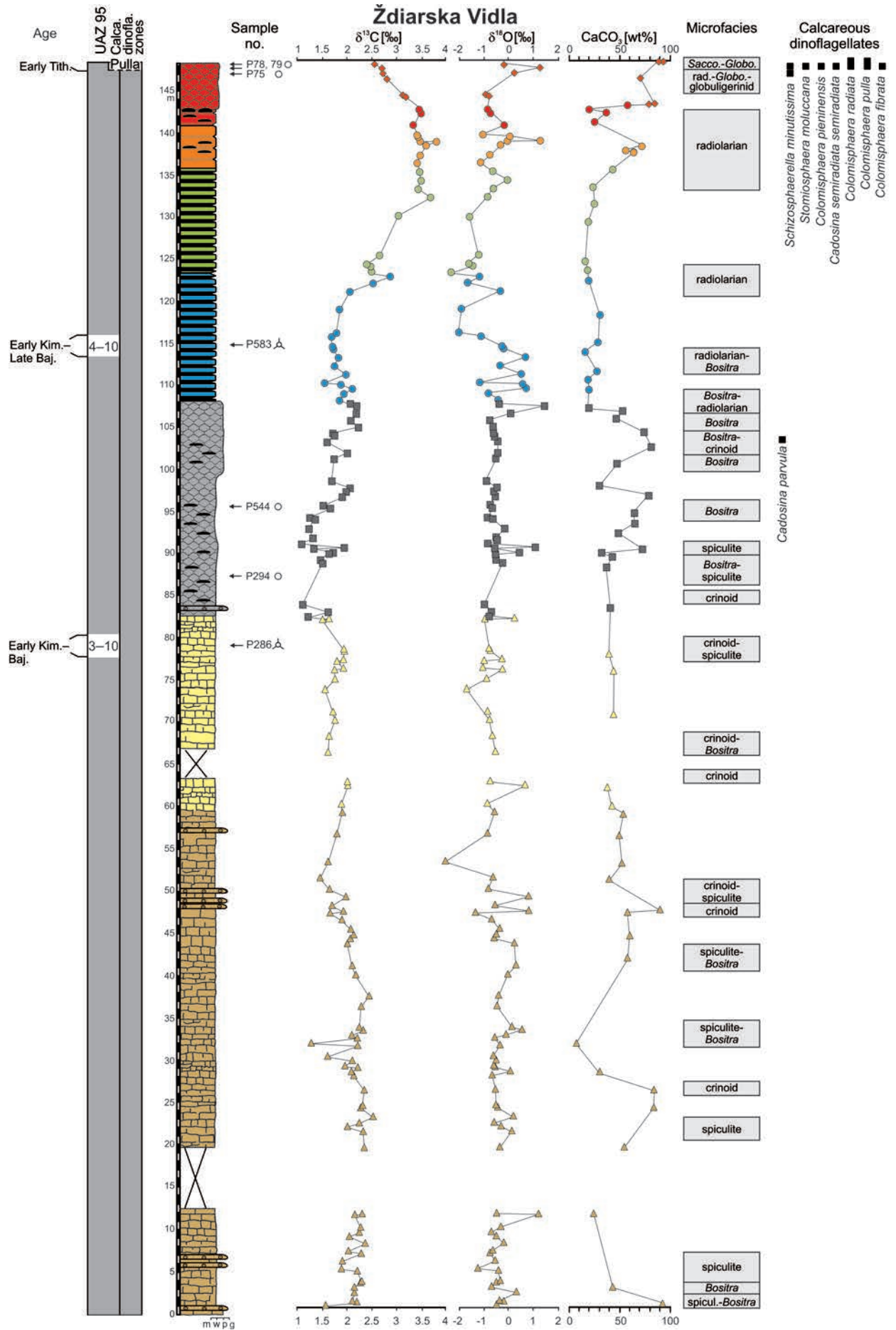
Fig. 7. Filipka Valley section in the High Tatra Mountains. Lithology, biostratigraphy (including position of the radiolarian and calcareous dinoflagellate samples) and results for carbon and oxygen isotope measurements, CaCO_3 content and microfacies analysis. Age denotes calibration of radiolarian (UAZ 95) or calcareous dinoflagellata zones. Legend for lithologies as in Fig. 3.

rian wackestone-packstone (Figs 3–8). These deposits contain calcified radiolarian tests, fragments of the shells of *Bositra*, *Saccocoma* sp. and tests of the planktonic foraminifer *Globuligerina* and sponge spicules, crinoids, cysts of calcareous dinoflagellates, ophiuroids and ostracods. The scarce macrofauna is represented by aptychi and belemnite rostra. Siliciclastic admixtures are represented by silt-sized grains of quartz and muscovite flakes.

Red nodular limestones

The red nodular limestones, 5.5–11 m thick, were assigned to the Czorsztyń Limestone Formation (Lefeld *et al.*, 1985). This facies occurs in all of the sections studied (Figs 3–8). The red nodular limestones show diverse lithotypes (Figs 3–8): (i) thin- and medium-bedded red limestones, al-

ternating with 1–2 cm-thick marls, locally with indistinct nodule development, and concentrations of aptychi (this lithotype bears a resemblance to the *Rosso ad Aptici* facies), (ii) massive nodular limestones, where light-coloured micritic nodules are surrounded by a distinct dark reddish to brownish clay-rich matrix with common dissolution seams, and (iii) highly calcareous nodular limestones, locally of brecciated type, with rounded or subangular nodules, separated by stylolites or dissolution seams. The first two lithotypes occur in the Western Tatra Mountains, the third one in the High Tatra and Belianske Tatra Mountains. Generally, nodule development becomes less common westward, which corresponds to a decrease in CaCO_3 content and thickness (Lefeld, 1974). This change reflects a lateral interfingering of the red nodular limestones westward (Czorsztyń Limestone Formation) with platy limestones (the Jasenina Formation),



containing red nodular packages. A greenish grey radiolarite bed with a thickness of 40 cm occurs in the nodular limestones in the Lejowa Valley section (Lc39; Fig. 4A, B). The average CaCO_3 content of red nodular limestones is about 67 wt%, ranging from 45 up to 97 wt% (Figs 3–8).

The nodular limestones contain *Bositra-Saccocoma* and *Saccocoma-Bositra*, *Saccocoma*-spiculite wackestone to packstone, *Saccocoma*, *Saccocoma*-radiolarian, radiolarian, radiolarian-globuligerinid-*Globochaete* wackestone microfacies (Figs 3–8). Moreover, the limestones contain fragments of foraminifera, calcified sponge spicules, aptychi, belemnites, crinoids, cysts of the calcareous dinoflagellates and the microproblematicum *Gemeridella minuta* Borza et Mišík. Silt-sized muscovite flakes and quartz grains are common, mostly in the parts that are rich in stylolites.

Platy limestones

Grey, platy limestones occur over the entire study area and represent the lower part of the Jasenina Formation (Michalík *et al.*, 1990). Light grey and olive-grey, partly siliceous, micritic limestones and marlstones predominate. Locally, they are reddish, pinkish and slightly nodular. The limestone beds are 2–10 cm thick. The average CaCO_3 content is 58 wt%, ranging from 46 to 72 wt%. Trace fossils are rare.

Four microfacies were distinguished (Figs 3, 4): *Saccocoma*, crinoid-*Saccocoma*, *Saccocoma*-radiolarian and *Saccocoma-Globochaete* wackestones. In addition, the bioclasts include spicules, filaments, ostracods, foraminifers, crinoids, bivalves, the microproblematicum *Gemeridella minuta* Borza et Mišík, and the cysts of calcareous dinoflagellates, the chitinoideidellids (Figs 3, 4). Gąsiorowski (1959, 1962) described the common occurrence of *Laevaptychus* sp. in the lowermost part of this facies.

SECTION DESCRIPTIONS AND STABLE-ISOTOPE RESULTS

The six sections of the Middle–Upper Jurassic deposits studied in the Tatra Mountains represent various tectonic units of the Krížna Nappe (Table 1). The sections are as follows from west to east (Fig. 1): Długa Valley (Dolina Długa), Lejowa Valley (Dolina Lejowa), Zadnia Kopka Kościeliska, Upląziańska Kopa, Filipka Valley (Dolina Filipka) and Ždiarska Vidla (Płaczliwa Skala in Polish). The first four sections are located in the Western Tatra Mountains, whereas two other ones in the High Tatra and Belianske Tatra Mountains, respectively.

Długa Valley section

The section is exposed in the Długa Valley, which is a tributary valley of the Chochołowska Valley (Dolina Chochołowska; Fig. 1; Table 1). The Middle–Upper Jurassic de-

posits crop out in a north-south-oriented shallow gully, running from the Pośrednie ridge to the bottom of the Długa Valley. The section is 71 m thick (Fig. 3).

The *Bositra*-crinoidal limestones (about 16 m) overlie the Lower Toarcian–?Aalenian red nodular limestones. Their lower part (1.7 m thick) consists of pink and grey condensed crinoidal limestones (Fig. 3), which towards the top gradually pass into the *Bositra* limestones (up to 14 m). The siliceous deposits start with spotted radiolarites, 9 m thick, which are succeeded by 4.5 m of green radiolarites. Contact between the green and variegated radiolarites is marked by a minor fault. The calcareous variegated radiolarites (12 m) are overlain by red radiolarites (4 m), which terminate the siliceous part of the section. In the Długa Valley section, the overlying red nodular limestones (5.5 m thick) are replaced by platy limestones of the Jasenina Formation, the uppermost 20 m of the section studied.

The 118 bulk carbonate samples from this 71 m section display significant variation in the $\delta^{13}\text{C}$ values. In the *Bositra*-crinoidal limestones, the interval from 0–15.5 m, the $\delta^{13}\text{C}$ curve shows values of 2.5‰, followed by relatively stable values of about 2‰ (Fig. 3). Towards the top, in the spotted radiolarites from 16–18.5 m, a negative $\delta^{13}\text{C}$ excursion is recorded, with values decreasing from 2‰ to a minimum value of 1.2‰. The minimum is followed by an increase in the $\delta^{13}\text{C}$ values to a maximum of 3.2‰, in green radiolarites at 28.4 m. Over the maximum the $\delta^{13}\text{C}$ values show almost constant decrease from 3.2‰ to 1.1‰. The only exception is a shift towards higher values in the order of 2.2‰ in the red nodular limestones of the interval 42–47 m.

Lejowa Valley section

This section is located on the slope of Pośrednia Kopka Hill (Fig. 1; Table 1). It is composed of three partial sections (L, Lb and Ld), with a measured thickness of 66 m (Fig. 4A). The lowermost part of the section (L) is exposed in a small rocky cliff on the southern slopes of Pośrednia Kopka Hill. The middle part of the section (Lb) is located at the southern margin of a forested gully, running towards the Huty Lejowe Glade (Polana Huty Lejowe). The uppermost part of the section (Ld) crops out in a rocky cliff. Section Lc is 11.5 m thick (Fig. 4B) and is situated at a rocky step in the axis of the gully.

The Toarcian–?Aalenian red nodular limestones with ferruginous macrooncooids are covered by the *Bositra*-crinoidal limestones (about 4 m, not fully exposed) studied, which are succeeded by slightly spotted radiolarites (about 12 m, not fully exposed) and green radiolarites (about 3.5 m; Fig. 4). The upper part of the section consists of variegated radiolarites, with reddish and greyish chert nodules (14 m), red radiolarites (about 9 m), massive, red nodular limestones (about 8 m) with a radiolarite intercalation 40 cm thick, and platy limestones with packages of red, slightly nodular limestones (about 20 m). Section Lc consists of red radiolarites (4.5 m), followed by red nodular limestones with a radiolarite bed (7 m).

Fig. 8. Ždiarska Vidla section in the Belianske Tatra Mountains. Lithology, biostratigraphy (including position of the radiolarian and calcareous dinoflagellate samples) and results for carbon and oxygen isotope measurements, CaCO_3 content and microfacies analysis. Age denotes calibration of radiolarian (UAZ 95) or calcareous dinoflagellata zones. Legend for lithologies as in Fig. 3.

Zadnia Kopka Kościeliska section

This section is situated on the eastern slope of Zadnia Kopka Kościeliska, which is a forested hill between the Lejowa and Kościeliska valleys (Fig. 1; Table 1). The section studied is 32 m thick (Pk; Fig. 5).

The lower part of the section comprises green radiolarites (0.9 m) and variegated radiolarites (at least 4 m). Above an exposure gap of 9 m, variegated radiolarites occur (14 m), followed by red radiolarites (3.6 m).

Uplaziańska Kopa section

The section crops out on the western slope of Uplaziańska Kopa Hill in the Western Tatra Mountains. Previously (Lefeld, 1974; Lefeld *et al.*, 1985; Polák *et al.*, 1998), the section was described under the name of Gładkie Uplaziańskie (Fig. 1; Table 1). The section is 34 m thick (Fig. 6).

The succession studied starts with green radiolarites (0.3 m) which pass into variegated radiolarites, with common massive red and dark grey chert nodules (17 m), red radiolarites (at least 2 m) and red nodular limestones (about 12 m; Fig. 6). The upper part of the section is poorly exposed, owing to thrust faulting.

The $\delta^{13}\text{C}$ values (54 samples) from the Uplaziańska Kopa section show a steady decrease of 2.2‰ (from 3.3‰ to 1.1‰). Only small maximum occurs (of 3.3‰) just below the boundary of green and variegated radiolarites.

Filipka Valley section

This section is located near the Filipczańska Glade (Filipczańska Polana), in the Filipka Valley, High Tatra Mountains (Fig. 1; Table 1). This section consists of three parts: Fp, Fz and Fk. The lowermost part (Fp) begins in a forested creek, which is a right tributary of the Filipczański Stream (Filipczański Potok). The partial sections Fz and Fk were studied and measured along the stream bed (waterfall) of the Filipczański Stream, with some vertical segments. The section is 89 m thick (Fig. 7); the beds are in an overturned position.

The section commences with spotted limestones with a measured thickness of 32 m (Fig. 7). In their uppermost part, siliceous radiolarian limestones occur (Iwańczuk *et al.*, 2013). They are replaced by grey nodular limestones (22 m). The spotted radiolarites (12 m) change to siliceous green radiolarites (about 6 m). The grey radiolarites are covered by variegated radiolarites (1 m, not fully exposed). The contact between the variegated and the red radiolarites is marked by a thrust fault. The red radiolarites (2 m thick), underlying the red nodular limestones, are calcareous and rich in red chert nodules. A transitional zone to the red nodular limestones exhibits red, elongated chert nodules. The red nodular limestones (13 m) are red, dusky red, pinkish and greyish pink.

The 45 bulk samples from the upper 60 m of the Filipka Valley section were analysed for stable isotope composition (Fig. 7). The $\delta^{13}\text{C}$ curve shows a slightly scattered pattern that probably results from the lower sampling resolution. In the uppermost part of the section (69–76 m), the maximum $\delta^{13}\text{C}$ values of 3.1‰ were documented in the green radio-

larites and as high as 3.4‰ in the variegated radiolarites. In the interval 76–89 m, the $\delta^{13}\text{C}$ values decrease from 3.5‰ to 1.6‰.

Ždiarska Vidla section

The section is situated on the eastern slope of Ždiarska Vidla Mountain (Płaczliwa Skała in Polish) in the Belianske Tatras Mountains in Slovakia (Fig. 1; Table 1). The lower part of the section crops out along the mountain path, leading to the top of the Ždiarska Vidla Mountain while its higher part is located on a rocky slope above the path. The section is 148 m thick (Fig. 8). Spotted limestones of the Łomy Limestone Member overlie the Middle Aalenian–lowermost Lower Bajocian black shales and limestones with *Bositra* (the Podskalnia Shale Member; Lefeld *et al.*, 1985; Iwańczuk *et al.*, 2013; see Fig. 17). The contact between these two Members exhibits considerable tectonic disturbance. For this reason, the lowermost part of the Łomy Limestone Member was not included in the study.

The lower part of the section comprises spotted limestones (spotted limestones and marls, 60 m thick, succeeded by 23 m of spotted limestones with cherts) with beds of crinoidal turbidites (Fig. 8; Mišík, 1959). The spotted limestones gradually pass into grey nodular limestones (25 m thick). The main part of the section consists of spotted radiolarites (15 m), green radiolarites (about 12 m), variegated radiolarites (5 m) and red radiolarites (about 2 m). The siliceous deposits are covered by red nodular limestones (about 10 m; measured thickness 5 m).

The 148 bulk samples from the Ždiarska Vidla section show considerable variation in $\delta^{13}\text{C}$ values (Fig. 8). A positive excursion in $\delta^{13}\text{C}$ values, with an amplitude of 1‰ and steady high values of about 2.5‰, is recorded in the spotted limestones (up to 38 m). In the interval 84–95 m, the $\delta^{13}\text{C}$ curve fluctuates slightly, reaching minimal values of about 1.1‰. In the interval 98–108 m, the $\delta^{13}\text{C}$ curve reaches its maximum with values of 2.2‰ at the top of the grey nodular limestones. In the spotted radiolarites, the $\delta^{13}\text{C}$ curve exhibits a minimum value of 1.7‰, followed by the main positive excursion of about 3.7‰. High $\delta^{13}\text{C}$ values of about 3.5‰ stay stable up to 142 m in the red radiolarites. In the overlying red nodular limestones, the $\delta^{13}\text{C}$ curve constantly decreases to minimum values of 2.5‰.

RADIOLARIAN DATING

The radiolarites of the Krížna Nappe contain some carbonate admixture and the radiolarians are usually calcified and not well preserved. Consequently, the extraction of radiolarians was often unsuccessful or the microfossils obtained had limited stratigraphic value, because of the poor state of preservation (see Ožvoldová, 1997). A list of species is given in Table 2 and species are illustrated in Figs 9–12. Radiolarians were analysed in all of the sections studied. The sample locations are shown in Figs 3–8.

Latest Bajocian to Early Callovian (UAZs 5–7) radiolarians were obtained from the spotted radiolarites (samples Fp143 and Fp269), in the middle part of the Filipka

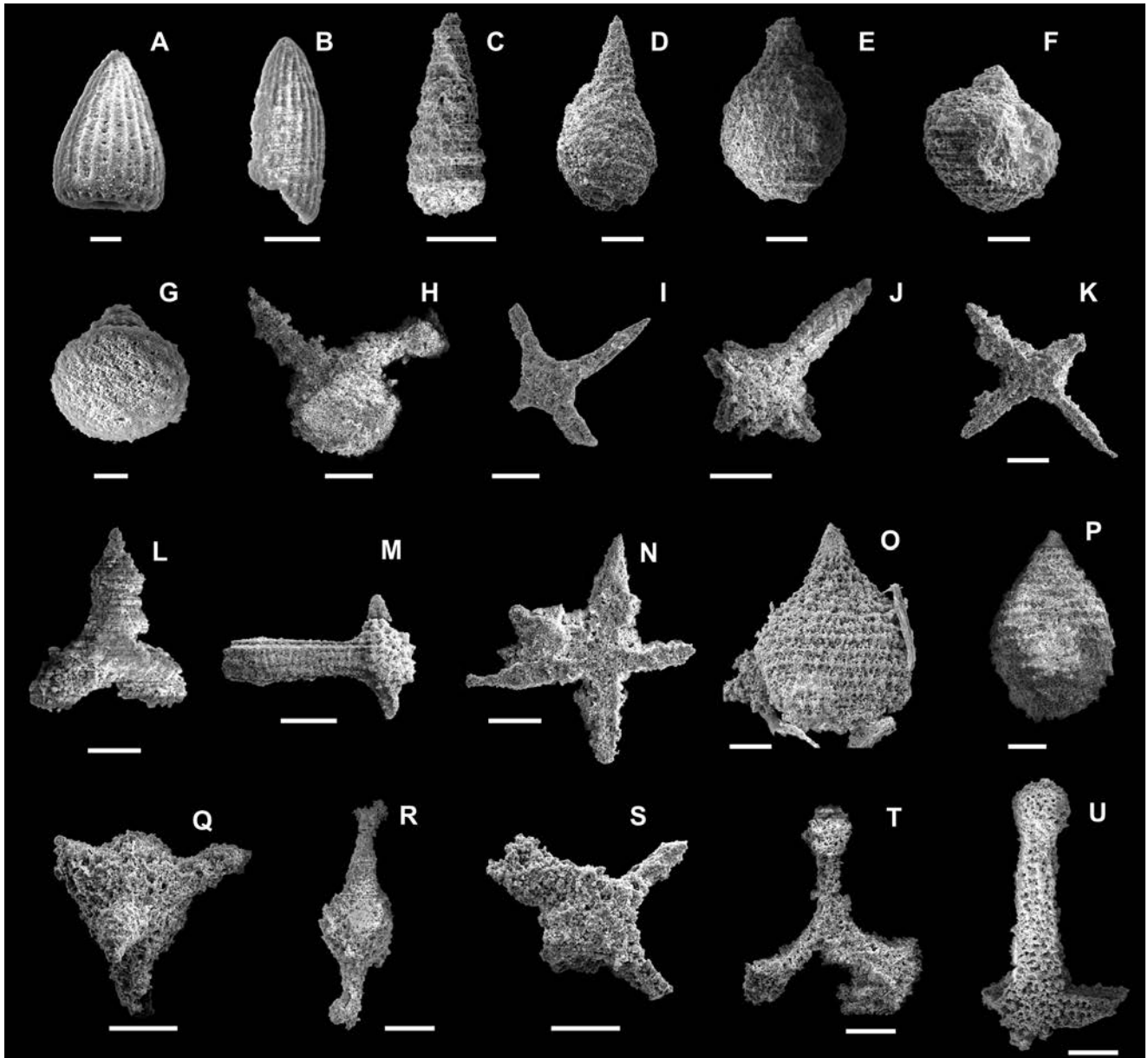


Fig. 9. Radiolarians from samples of the Długa Valley section (Dsr). Scale bars in A, G = 20 μm , in B, F = 50 μm , in C–E, H–U = 100 μm . Figs A–G. Sample Dsr62; latest Bajocian–Early Bathonian to Early Oxfordian (UAZs 5–8). **A.** *Archaeodictyomitra patricki* Kocher. **B.** *Archaeodictyomitra whalena* Kozur et Mostler. **C.** *Cinguloturris?* sp. **D.** *Mirifusus fragilis* Baumgartner. **E.** *Mirifusus guadalupensis* Pessagno. **F.** *Zhamoidellum* sp. **G.** *Hemicryptocapsa* cf. *yaoi* (Kozur). Figs H–N. Sample Dsr96; Middle to Late Oxfordian (UAZs 6–9). **H.** *Bernoullius rectispinus* s.l. Kito, De Wever, Danelian et Cordey. **I.** *Emiluvia sedecimporata* (Rüst). **J.** *Emiluvia* cf. *salensis* Pessagno. **K.** *Emiluvia* sp. **L.** *Paronaella* cf. *mulleri* Pessagno. **M.** *Monotrabs goricanae* Beccaro. **N.** *Tetraditryma corralitosensis* (Pessagno). Figs O–U. Sample Dsr203; Middle Oxfordian to Early Tithonian (UAZs 9–11). **O.** *Mirifusus guadalupensis* Pessagno. **P.** *Mirifusus* sp. **Q.** *Parapodocapsa amphitrepera* (Foreman). **R.** *Spinocapsa* cf. *spinosa* (Ožvoldová). **S.** *Emiluvia* sp. **T.** *Angulobracchia* cf. *biordinalis* Ožvoldová. **U.** *Tetratrabs bulbosa* Baumgartner.

Valley section (Fig. 7). Both assemblages (Fig. 12A–O) indicate UAZs 5–7; the assemblage in sample Fp143 contains *Palinandromeda podbielensis* (Ožvoldová) (FAD = First Appearance Datum in UAZ 5), together with *Belleza decora* (Rüst) (LAD = Last Appearance Datum in UAZ 7). The genus *Semihsuum*, last appearing in the Late Callovian (O’Dogherty *et al.*, 2009), was also found. The presence of *Zhamoidellum ovum* Dumitrica (FAD in Callovian, Suzuki *et al.*, 2001) could indicate a more restricted age for sample Fp143 that is not older than the Early Callovian. The overly-

ing sample Fp269 lacks *Semihsuum*, but contains *Belleza decora* (Rüst). This species was assumed to be restricted to UAZs 4–7 (Baumgartner *et al.*, 1995), but Marcucci and Prela (1996) suggested that the species could reach the Early Oxfordian (UAZ 8). Thus it is possible that sample Fp269 is somewhat younger than Callovian.

Latest Bajocian to Early Oxfordian (UAZs 5–8) radiolarians were found in the spotted radiolarites of the Długa Valley section (sample Dsr62; Fig. 3) and in the lower part of the Lejowa Valley section (sample L58; Fig. 4). Sam-

Table 2

Occurrence of radiolarian species in samples from the Middle-Upper Jurassic deposits of the Křížna Nappe, Tatra Mountains

Section		Długa Valley			Lejowa Valley						ZKK	Uplazińska Kopa		Filipka Valley		Ždiarska Vidla	
Species	Sample	Dsr	DsR	Dsr	L58	L140	Lb1	L183	Lb38	Lc39	Pk35	Gd7	Gd21	Fp143	Fp269	P286	P583
	UAZ95	62	96	203													
<i>Angulobracchia</i> sp.												x					
<i>Angulobracchia biordinalis</i> Ožvoldová	9–11			cf.													
<i>Arcanica</i> <i>funatoensis</i> (Aita)	3–11												cf.				
<i>Archaeodictyomitra patricki</i> Kocher		x									x						
<i>Archaeodictyomitra whalenae</i> Kozur et Mostler		x															
<i>Archaeodictyomitra</i> sp.										x			x				
<i>Belleza decora</i> (Rüst)	4–7													x	x		
<i>Bernoullius rectispinus</i> s.l. Kito, De Wever, Danelian et Cordey	1–9		x		x												
<i>Cinguloturris</i> sp.		x					x										
<i>Emiluvia ordinaria</i> Ožvoldová	9–11					x											
<i>Emiluvia orea</i> Baumgartner	4–11					x											
<i>Emiluvia salensis</i> Pessagno	4–13		cf.														
<i>Emiluvia sedecimporata</i> (Rüst)	3–11		x														
<i>Emiluvia</i> sp.			x	x	x						x						
<i>Hemicryptocapsa carpathica</i> (Dumitrica)	7–11						cf.										
<i>Hemicryptocapsa yaoi</i> (Kozur)		cf.															
<i>Higumastra</i> sp.												x					
<i>Higumastra imbricata</i> (Ožvoldová)	4–8				cf.									x			
<i>Hiscocapsa lugeoni</i> O'Dogherty, Goričan et Dumitrica														x			
<i>Hiscocapsa</i> sp.							x			x					x		
<i>Homoeoparoneaella argolidensis</i> Baumgartner	4–11													cf.	cf.		
<i>Homoeoparoneaella pseudoewingi</i> Baumgartner	3–7														cf.		
<i>Lanubus cornutus</i> (Baumgartner)	8–10										cf.						
<i>Mirifusus diana</i> s.l. (Karrer)	7–20			cf.						x							
<i>Mirifusus fragilis</i> s.l. Baumgartner	3–8	x												cf.			
<i>Mirifusus guadalupensis</i> Pessagno	5–11	x	cf.	x	x						x			x			
<i>Mirifusus</i> sp.				x													
<i>Monotrabs goricana</i> Beccaro			x		cf.												
<i>Obesacapsula morroensis</i> Pessagno	5–21			x	x												
<i>Obesacapsula</i> sp.			x											x			
<i>Olanda</i> sp.														x			
<i>Palinandromeda podbielensis</i> (Ožvoldová)	5–9													x			
<i>Parapodocapsa amphitrepta</i> (Foreman)	9–18			x													
<i>Paronaella mulleri</i> Pessagno	6–10		cf.														
<i>Paronaella</i> sp.					x							x					x
<i>Praewillriedelum convexum</i> (Yao)	1–11														x		
<i>Semihsuum rutogense</i> (Yang et Wang)														x			
<i>Spinocapsa spinosa</i> (Ožvoldová)	8–13			cf.													
<i>Spinocapsa</i> sp.										x					x		x

Table 2 continued

Section	Sample	Długa Valley			Lejowa Valley						ZKK	Uptazińska Kopa		Filipka Valley		Ždiarska Vidla	
		Dsr 62	Dsr 96	Dsr 203	L58	L140	Lb1	L183	Lb38	Lc39	Pk35	Gd7	Gd21	Fp 143	Fp 269	P286	P583
<i>Spongocapsula perampla</i> (Rüst)	6–11							cf.									
<i>Tetrarabs bulbosa</i> Baumgartner	7–11			x													
<i>Tetradityma corralitosensis</i> (Pessagno)	3–10		x														
<i>Tetradityma pseudoplena</i> Baumgartner	4–11												cf.				cf.
<i>Transhsuum maxwelli</i> gr. (Pessagno)	3–10															x	
<i>Transhsuum</i> sp.					x												
<i>Triactoma blakei</i> (Pessagno)	4–11				x	x											
<i>Triactoma jonesi</i> (Pessagno)	2–13				x												
<i>Triactoma</i> sp.								x		x		x					
<i>Trirabs casmaliaensis</i> (Pessagno)	4–10											x					
<i>Trirabs ewingi</i> s.l. (Pessagno)	4–22				x												
<i>Trirabs exotica</i> (Pessagno)	4–11					x											
<i>Trirabs rhododactylus</i> Baumgartner	3–13					x											
<i>Trirabs</i> sp.													x				x
<i>Williriedellum</i> sp.						x											
<i>Zhamoidellum ovum</i> Dumitrica	?7–11							x	x	cf.				x			
<i>Zhamoidellum</i> sp.		x				x			x		x			x			
Age (UAZones 95)		5–8	6–9	9–11	5–8	9–11	9–11	9–11	9–11	9–11	8–10	4–10	4–11	5–7	5–7	3–10	4–10
Facies		sr	gr	rr	sr	vr	vr	vr	rr	rnl	vr	gr	vr	sr	sr	cl	sr

The second column gives the zonal ranges of the species according to Baumgartner et al. (1995). Lithology: cl – cherty limestones, sr – spotted radiolarites, gr – green radiolarites, vr – variegated radiolarites, rr – red radiolarites, rnl – red nodular limestones

ple Dsr62 yielded a badly preserved radiolarian association (Fig. 9A–G). Its age is determined on the basis of the presence of *Mirifusus fragilis* Baumgartner (LAD in UAZ 8) and *Mirifusus guadalupensis* Pessagno (FAD in UAZ 5). Sample L58 (Fig. 10A–K) is constrained with *Higumastra imbricata* (Ožvoldová) (LAD in UAZ 8), *Obesacapsula morroensis* Pessagno and *Mirifusus guadalupensis* Pessagno (FADs in UAZ 5).

Middle Bathonian to Middle–Late Oxfordian (UAZs 6–9) radiolarian assemblage was obtained from green radiolarites of the Długa Valley sections (sample Dsr96; Figs 3, 9H–N). The age assignment is based on the first occurrence of *Paronaella mulleri* Pessagno (UAZ 6) and the last occurrence of *Bernoullius rectispinus* s.l. Kito, De Wever, Danejian et Cordey (UAZ 9).

Middle Callovian to Early Kimmeridgian (UAZs 8–10) radiolarians were identified in the lower part of variegated radiolarites of the Zadnia Kopka Kościeliska section (Fig. 5). Sample Pk35 yielded many and relatively diverse radiolarians (Fig. 11A–F). The age is based on the range of *Janubus cornutus* (Baumgartner) (UAZs 8–10).

Middle Oxfordian to Early Tithonian (UAZs 9–11) radiolarians were identified in the red radiolarites of the upper part of the Długa Valley section (sample Dsr203; Fig. 3), in the uppermost part of the variegated radiolarites, red radiolarites, red nodular limestones of the Lejowa Valley section (sample Lb1, L183, Lb38 and Lc39; Fig. 4) and

from the variegated radiolarites of the middle part (L140). According to the presence of *Angulobracchia biordinalis* Ožvoldová (UAZs 9–11) sample Dsr203 (Fig. 9O–U) is of a Middle Oxfordian to Early Tithonian age.

The assemblage in sample L140 (Fig. 10L–Q) is characterized by the presence of *Emiluvia ordinaria* Ožvoldová (UAZs 9–11). The uppermost radiolarian sample from the same section (Lb38) is not younger than Early Tithonian, as evidenced by *Zhamoidellum ovum* Dumitrica (LAD in UAZ 11). All four successive samples in the variegated and red radiolarites (L140, Lb1, L183, and Lb38; Fig. 10L–X) thus are assigned to the interval UAZs 9–11. The sample Lc39 (Fig. 10Y–AB), from the base of the red nodular limestones in a parallel section, also contains *Zhamoidellum ovum* Dumitrica and hence is not younger than UAZ 11. On the basis of the local correlation between the two sections in the Lejowa Valley, sample Lc39 is assigned to UAZs 9–11.

The assemblages in some samples (P286, P583, Gd7, Gd21) allow only a very broad age assignment. In sample P286 (from the lower part of the Ždiarska Vidla section, Figs 8, 11R), an Early Bajocian–Early Kimmeridgian age (UAZs 3 to 10) could be inferred on the basis of *Transhsuum maxwelli* gr. (Pessagno). Sample P583 (the spotted radiolarites of the middle part of the Ždiarska Vidla section, Figs 8, 11N–Q) is characterized by relative abundance of small undeterminable nassellarians. A Late Bajocian to Early Kimmeridgian age (UAZs 4 to 10) of the sample P583 is in-

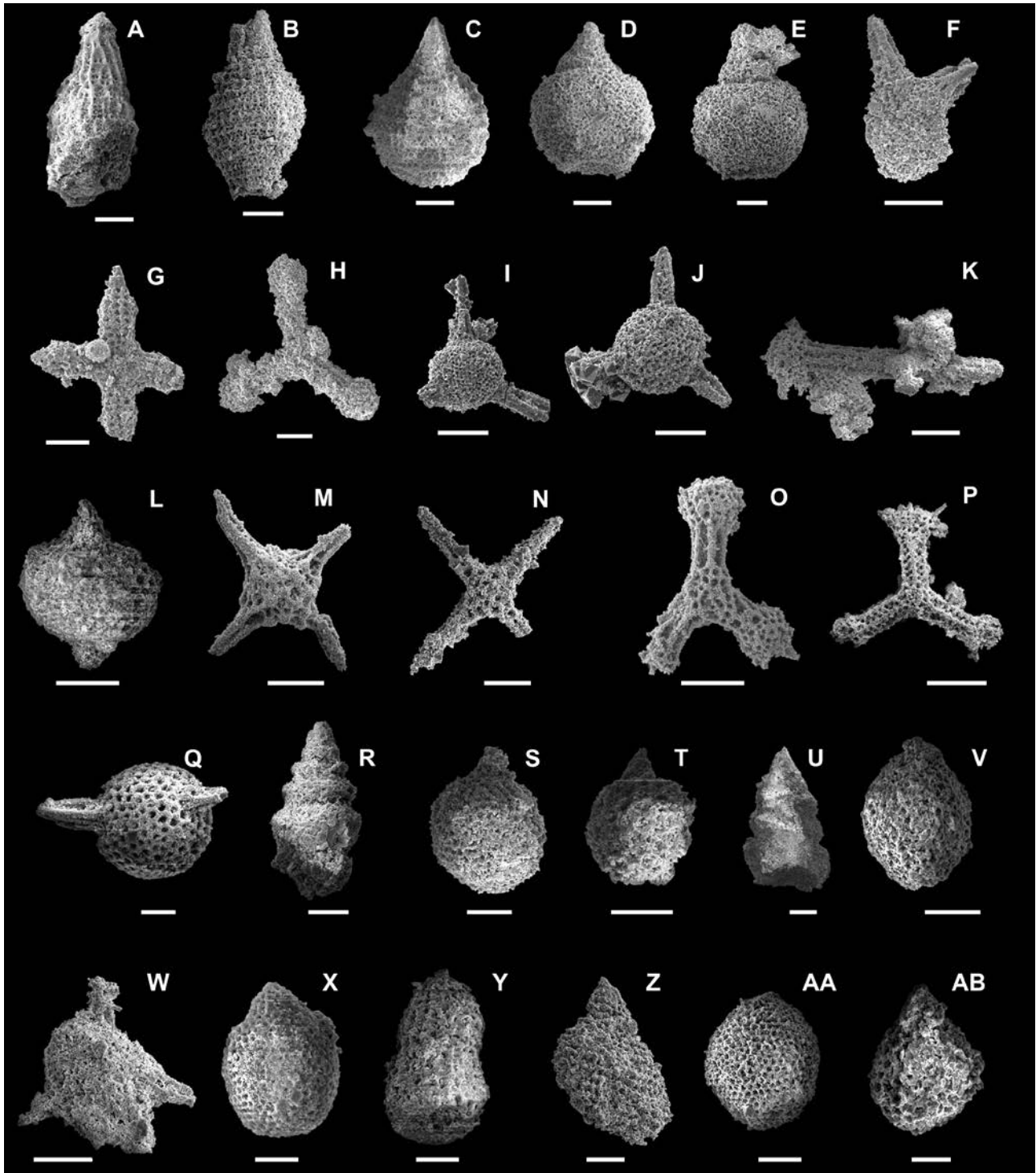


Fig. 10. Radiolarians from samples of the Lejowa Valley section (L, Lb, Lc). Scale bars in A, Q, X, Y, AB = 50 μm , in FB–P, R–Z, AA = 100 μm . Figs A–K. Sample L58; Latest Bajocian–Early Bathonian to Early Oxfordian (UAZs 5–8). **A.** *Transsuum* sp. **B.** *Mirifusus guadalupensis* Pessagno. **C.** *Mirifusus* cf. *guadalupensis* Pessagno. **D.** **E.** *Obesacapsula morroensis* Pessagno. **F.** *Bernoullius rectispinus* s.l. Kito, De Wever, Danelian et Cordey. **G.** *Higumastra* cf. *imbricata* (Ožvoldová). **H.** *Tritrabs ewingi* s.l. (Pessagno). **I.** *Triactoma jonesi* (Pessagno). **J.** *Triactoma blakei* (Pessagno). **K.** *Monotrabs* cf. *goricanae* Beccaro. Figs L–Q. Sample L140; Middle–Late Oxfordian to Late Kimmeridgian–Early Tithonian (UAZs 9–11). **L.** *Williriedellum* sp. **M.** *Emiluvia orea* Baumgartner. **N.** *Emiluvia ordinaria* Ožvoldová. **O.** *Tritrabs exotica* (Pessagno). **P.** *Tritrabs rhododactylus* Baumgartner. **Q.** *Triactoma blakei* (Pessagno). Figs R–T. Sample Lb1; Middle–Late Oxfordian to Late Kimmeridgian–Early Tithonian (UAZs 9–11). **R.** *Cinguloturris* sp. **S.** *Hemicryptocapsa* cf. *carpathica* (Dumitrica). **T.** *Hiscocapsa* sp. Figs U–W. Sample L183; Middle–Late Oxfordian to Late Kimmeridgian–Early Tithonian (UAZs 9–11). **U.** *Spongocapsula* cf. *perampla* (Rüst). **V.** *Zhamoidellum ovum* Dumitrica. **W.** *Triactoma* sp. Fig X. Sample Lb38; Middle–Late Oxfordian and Late Kimmeridgian–Early Tithonian (UAZs 9–11). **X.** *Zhamoidellum ovum* Dumitrica. Figs Y–AB. Sample Lc39; Middle–Late Oxfordian to Late Kimmeridgian–Early Tithonian (UAZs 9–11). **Y.** *Archaeodictyomitra* sp. **Z.** *Mirifusus dianae* s.l. (Karrer). **AA.** *Zhamoidellum* cf. *ovum* Dumitrica. **AB.** *Hiscocapsa* sp.

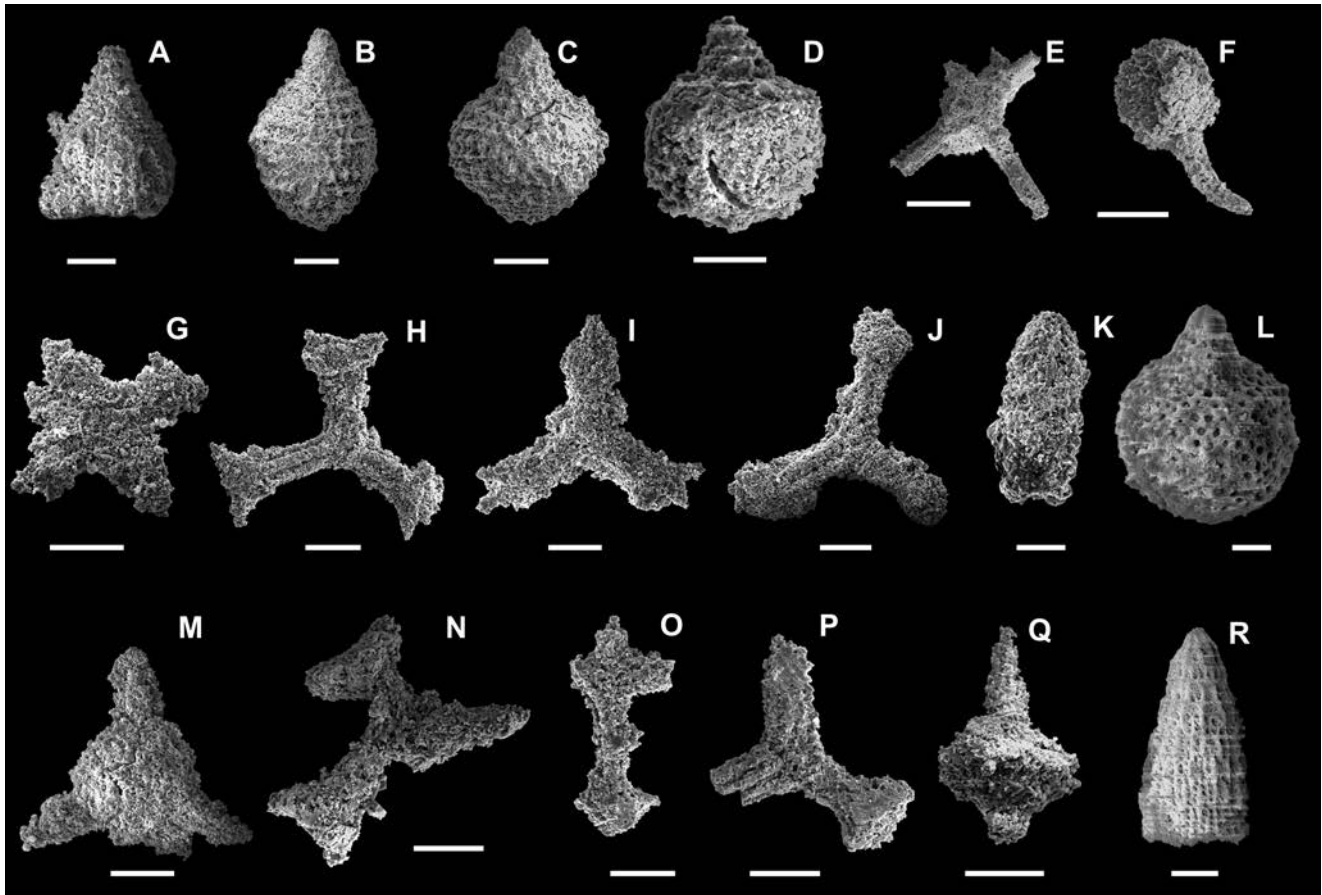


Fig. 11. Radiolarians from samples of the Zadnia Kopka Kościeliska section (Pk), Uplaziańska Kopa section (Gd) and Ždiarska Vidla section (P). Scale bars in L = 20 μm , in A, D, K = 50 μm , in B, C, E–J, M–R = 100 μm . Figs A–F. Sample Pk35; Middle Callovian–Early Oxfordian to Late Oxfordian–Early Kimmeridgian (UAZs 8–10). **A.** *Archaeodictyomitra patricki* Kocher. **B, C.** *Mirifusus guadalupensis* Pessagno. **D.** *Zhamoidellum?* sp. **E.** *Emiluvia* sp. **F.** *Lanubus* cf. *cornutus* (Baumgartner). Figs G–J. Sample Gd7; Late Bajocian to Late Oxfordian–Early Kimmeridgian (UAZs 4–10). **G.** *Higumastra* sp. **H.** *Tritrabs casmaliaensis* (Pessagno). **I.** *Paronaella* sp. **J.** *Angulo-bracchia* sp. Figs K–M. Sample Gd21; Late Bajocian to Late Kimmeridgian–Early Tithonian (UAZs 4–11). **K.** *Archaeodictyomitra* sp. **L.** *Arcanica* cf. *funatoensis* (Aita). **M.** *Triactoma* sp. Figs N–Q. Sample P583; Late Bajocian to Late Kimmeridgian–Early Tithonian (UAZs 4–11). **N.** *Paronaella* sp. **O.** *Tetraditryma* cf. *pseudoplana* Baumgartner. **P.** *Tritrabs* sp. **Q.** *Spinosicapsa?* sp. Fig. R. Sample P286; Early Bajocian to Early Kimmeridgian (UAZs 3–10). **R.** *Transhsuum maxwelli* gr. (Pessagno).

indicated by *Tetraditryma pseudoplana* Baumgartner (Fig. 11O). From the presence of *Tritrabs casmaliaensis* (Pessagno), sample Gd7 (lower part of the Uplaziańska Kopa section, Figs 6, 11G–J) is of Late Bajocian–Early Kimmeridgian age (UAZs 4–10). Sample Gd21 (lower part of the Uplaziańska Kopa section; about 2 m above sample Gd7; Fig. 11 K–M) is not younger than Late Kimmeridgian–Early Tithonian, as evidenced by *Arcanica funatoensis* (Aita) (UAZs 3–11).

CALCAREOUS DINOFLAGELLATE AND CALPIONELLID DATING

The biostratigraphy of the Kimmeridgian and Early Tithonian deposits studied is based on the calcareous dinoflagellate and calpionellid succession (see Jach *et al.*, 2012). Cysts of the calcareous dinoflagellates are generally well preserved, even if the matrix is recrystallized (Fig. 13). Six

dinocyst zones and one calpionellid zone were recognized in the sections studied (Figs 3–8).

The occurrence of the calcareous dinocyst association *Stomiosphaera moluccana* Wanner, *Cadosina parvula* Nagy, *Colomisphaera nagyi* (Borza), *C. carpathica* Borza, *C. pininiensis* (Borza), *Schizosphaerella minutissima* (Colom) was observed in the uppermost part of the red radiolarites and/or in the red nodular limestones of the Długa Valley (samples Dsr231–302a), Lejowa Valley (samples Lb44–88), Zadnia Kopka Kościeliska (sample Pk201) and Filipka Valley sections (sample Fz2; Figs 3–5, 7, 13A–B). This association is typical of the Late Kimmeridgian Moluccana Zone.

Younger deposits, the red nodular limestone of the Lejowa Valley (samples Lb91, 100, Lc17–39) and Filipka Valley sections (sample Fk37), yield a cyst association, with *Stomiosphaera moluccana* Wanner accompanied by *Carpistomiosphaera borzai* (Nagy) (Figs 4, 7, 13C). The latter cyst is the index marker of the Borzai Zone, which dates the topmost part of the Late Kimmeridgian (Lakova *et al.*,

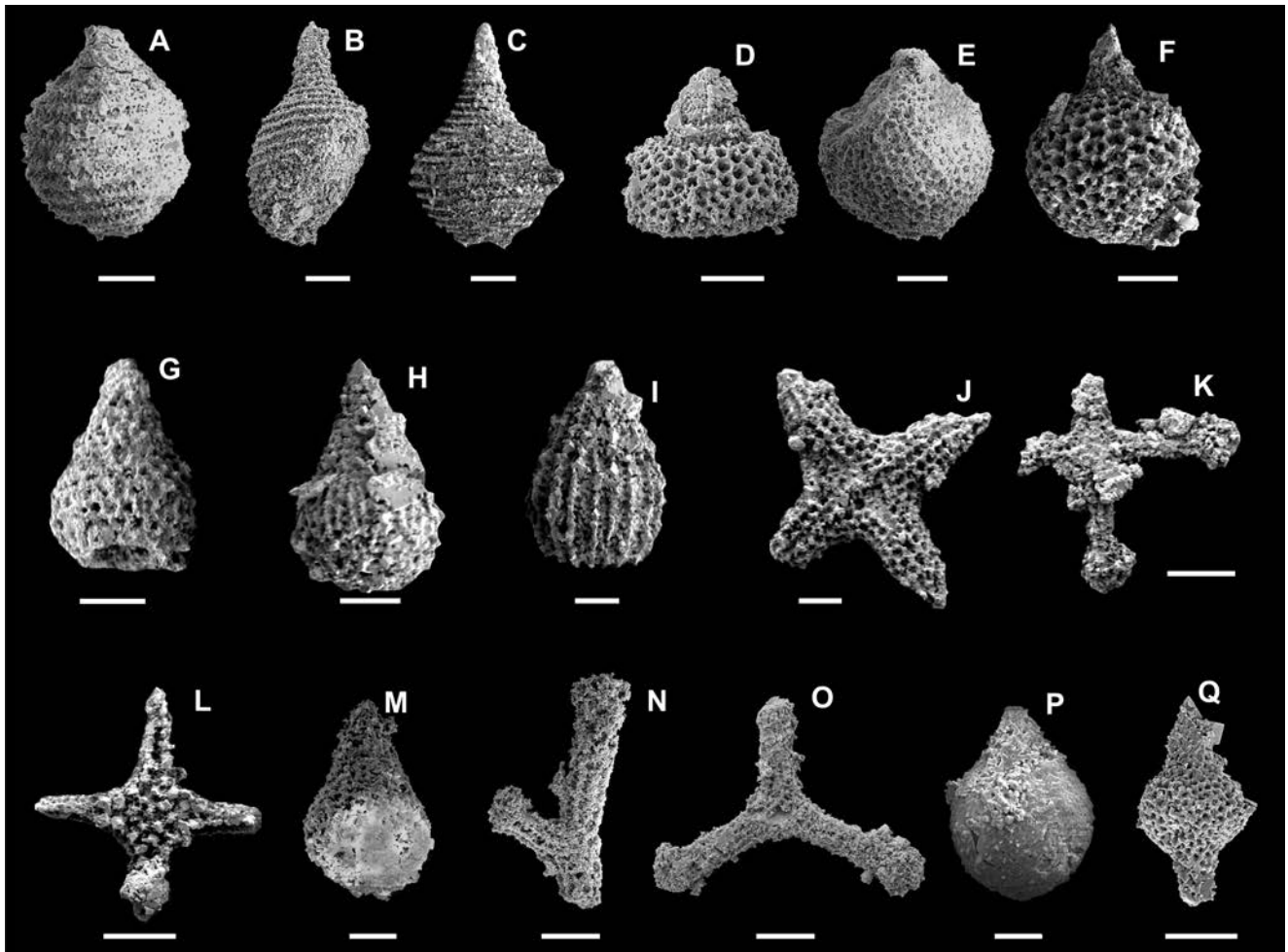


Fig. 12. Radiolarians from samples of the Filipka Valley section (Fp). Scale bars in G–J, M, P = 50 μm , in A–F, K, L, N, O = 100 μm . Figs A–L. Sample Fp143; Latest Bajocian–Early Bathonian to Late Bathonian–Early Callovian (UAZs 5–7). **A.** *Mirifusus guadalupensis* Pessagno. **B, C.** *Mirifusus* cf. *fragilis* Baumgartner. **D.** *Palinandromeda podbielensis* (Ožvoldová). **E.** *Zhamoidellum ovum* Dumitrica. **F.** *Olanda* sp. **G.** *Hiscocapsa lugeoni* O’Dogherty, Goričan et Dumitrica. **H.** *Belleza decora* (Rüst). **I.** *Semihsuum rutogense* (Yang et Wang). **J.** *Higumastra imbricata* (Ožvoldová). **K.** *Tetraditryma* cf. *pseudoplana* Baumgartner. **L.** *Emiluvia* sp. Figs M–O. Sample Fp269; Latest Bajocian–Early Bathonian to Late Bathonian–Early Callovian (UAZs 5–7). **M.** *Belleza decora* (Rüst). **N.** *Homoeoparonaella* cf. *pseudoewingi* Baumgartner. **O.** *Homoeoparonaella* cf. *argolidensis* Baumgartner. Fig. P. Sample Fp288. **P.** *Preawilliriedellum convexum* (Yao). Fig. Q. Sample Fk54. **Q.** *Spinocapsa* sp.

1999; Reháková, 2000) or according to older authors it dates the Late Kimmeridgian and earliest Tithonian (Nowak, 1968; Borza, 1984).

The overlying limestones – the middle or uppermost part of the red nodular limestones and/or the platy limestones of the Długa Valley (samples Dsr304–308), Lejowa Valley (samples Lb108–132a, Ld1, Ld5) and Ždiarska Vidla sections (samples P78, P79) – contain a cyst association with *Carpistomiosphaera borzai* (Nagy), *Colomisphaera pulla* (Borza), *C. radiata* (Vogler), *C. carpathica* (Borza), *C. pieniniensis* (Borza), *C. nagyi* (Borza), *Schizosphaerella minutissima* (Colom), *Stomiosphaera moluccana* Wanner, *Cadosina semiradiata semiradiata* Wanner and *Colomisphaera* aff. *fortis* Řehánek (Figs 3, 4, 8, 13D–G, K). This association marks the base of the Early Tithonian Pulla Zone. It should be noted that the last mentioned cyst shows a relation to *Colomisphaera fortis* (Řehánek), the zonal marker for the stratigraphically higher Fortis Zone (Řehá-

nek, 1992). But, in order to accept and make a correction to this cyst distribution and also a possible zonal scheme in the future, additional information is needed.

Despite the fact that one cyst resembles *Carpistomiosphaera tithonica* Nowak, the Pulla–Tithonica Zone of the Early Tithonian (*sensu* Lakova *et al.*, 1999; Reháková, 2000) was distinguished in the red nodular limestones of the Uplaziańska Kopa (sample Gd97) and Filipka Valley sections (sample Fk20). According to Borza (1984), *Carpistomiosphaera tithonica* Nowak (Figs 6, 7, 13H) and *Colomisphaera pulla* (Borza), occasionally may replace each other and are suitable for the recognition of the combined Pulla–Tithonica Zone (Early Tithonian).

The youngest cyst zone was determined in the uppermost part of the red nodular limestones and/or in the platy limestones of the Długa Valley (samples Dsr310–322a), Lejowa Valley (samples Lb135–146, Lc48), Uplaziańska Kopa (samples Gd100–128) and Filipka Valley (samples Fk

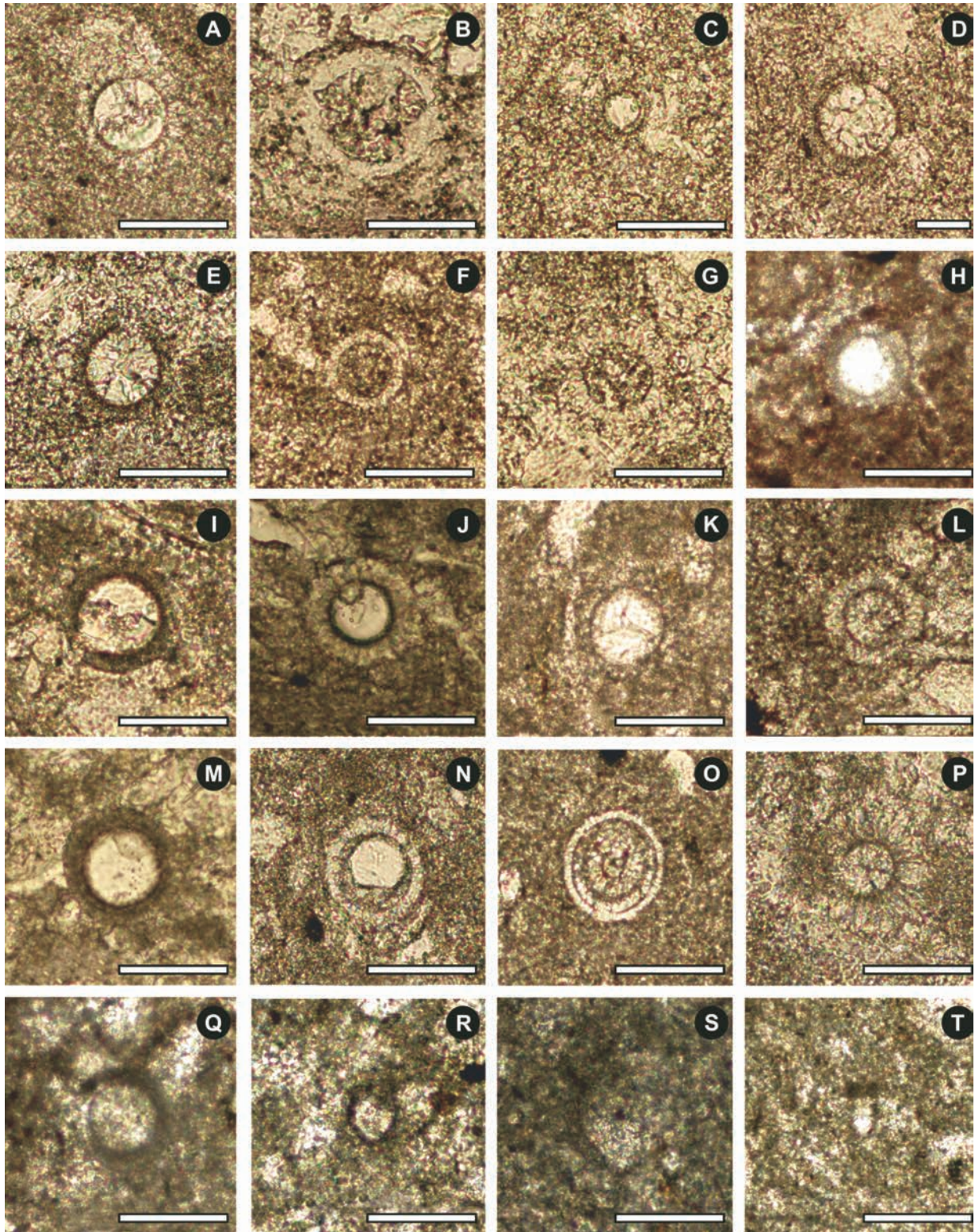


Fig. 13. Late Kimmeridgian–Early Tithonian calcareous dinoflagellates and chitinoideids. Sample locations in the sections are indicated in Figs 3–8. Scale bars: = 50 μm . **A.** *Colomisphaera nagyi* (Borza), sample Pk181. **B.** *Stomiosphaera moluccana* Wanner, sample Fz2. **C.** *Carpistomiosphaera borzai* (Nagy), sample Fk37. **D.** *Colomisphaera radiata* (Vogler), sample P78. **E.** *Colomisphaera pulla* (Borza), sample P78. **F.** *Schizosphaerella minutissima* (Colom), sample P78. **G.** *Schizosphaerella minutissima* (Colom), sample Fk20. **H.** *Carpistomiosphaera tithonica* Nowak, sample Gd97b. **I.** *Colomisphaera pulla* (Borza), sample Dsr312b. **J.** *Colomisphaera carpathica* (Borza), sample Dsr314. **K.** *Colomisphaera* aff. *fortis* (Borza), sample Dsr318a. **L.** *Colomisphaera carpathica* (Borza), sample Fk4. **M.** *Carpistomiosphaera tithonica* Nowak, sample Dsr312b. **N.** *Parastomiosphaera malmica* (Borza), sample Dsr314. **O.** *Parastomiosphaera malmica* (Borza), sample Fk1. **P.** *Colomisphaera cieszynica* (Borza), sample Dsr314. **Q.** *Cadosina semiradiata semiradiata* (Wanner), sample Gd146. **R.** *Borziella slovenica* (Borza), sample Ld12b. **S.** *Chitinoideella boneti* Doben, sample Ld12. **T.** *Longicollaria dobeni* (Borza), sample Ld12b.

1–9) sections. Here the cysts *Parastomiosphaera malmica* (Borza), *Schizosphaerella minutissima* (Colom), *Carpistomiosphaera tithonica* Nowak, *Stomiosphaera moluccana* Wanner, *Cadosina semiradiata semiradiata* Wanner, *Colomisphaera nagy* (Borza), *C. pulla* (Borza), *C. carpathica* (Borza), *C. cieszynica* (Borza), *C. pieniniensis* (Borza), *C. fibrata* (Nagy), *C. aff. fortis* Řehánek, and *C. radiata* (Vogler) were documented (Figs 3, 4, 6, 7, 13I–P). This cyst association is typical of the Malmica Zone (Early Tithonian). Since *Colomisphaera fibrata* (Nagy) was not observed in higher cyst zones up to now, its presence here can be considered to be the result of resedimentation. So far, the last occurrence of *Colomisphaera radiata* (Vogler) was identified in the Pulla Zone (Borza, 1984; Reháková, 2000). Thus, the stratigraphic range of this taxon should be corrected and shifted to the Malmica Zone.

Locally, in the Uplazińska Kopa section (samples Gd 133–146), the red nodular limestones contain a cyst association with frequent *Cadosina semiradiata semiradiata* Wanner (Figs 6, 13Q), *C. semiradiata fusca* (Wanner), *Schizosphaerella minutissima* (Colom) and *Colomisphaera cieszynica* (Borza). This association marks the base of the Early Tithonian Semiradiata Zone.

The first calpionellids with microgranular calcite loricas are *Borziella slovenica* (Borza) (Fig. 13R), *Chitinoidea boneti* Doben (Fig. 13S), *Longicollaria dobeni* (Borza) (Fig. 13T), *Dobeniella colomi* (Borza), occurring in the platy limestones of the Lejowa Valley section (samples Ld10, Ld12; Fig. 4), confirm the onset of the Early Tithonian Dobeni and the Boneti subzones of the Chitinoidea Zone (*sensu* Borza, 1984; Reháková, 2002; Jach *et al.*, 2012).

DISCUSSION

Stable-isotope stratigraphy

Imprint of diagenesis

Assessment of the influence of diagenetic alteration on the stable-isotope record in the deposits studied is necessary for any evaluation of their usefulness in chemostratigraphic correlation. Oxygen isotopes in carbonate deposits are susceptible to diagenetic alteration, owing to the much higher oxygen contents of diagenetic waters, compared to their (dissolved) carbon concentrations. As a consequence, the carbon isotopic record is less susceptible to alteration by burial diagenesis than the oxygen record (e.g., Banner and Hanson, 1990; Marshall, 1992). Usually, the rock-fluid alteration during diagenesis results in a decrease of $\delta^{18}\text{O}$ values, whereas diagenetic modification of $\delta^{13}\text{C}$ values may remain insignificant (e.g., Marshall, 1992; Padden *et al.*, 2002; Bojanowski *et al.*, 2014).

The $\delta^{13}\text{C}$ values of the analysed deposits range from 1 to 3.8‰, which is typical of Jurassic pelagic carbonates (e.g., Jenkyns and Clayton, 1986). All of the carbon-isotope curves generated show an agreement in the overall pattern. The $\delta^{13}\text{C}$ signal appears to be partly lithologically dependent as the major $\delta^{13}\text{C}$ excursions are found in biosiliceous facies (radiolarites). This can be explained by the primary,

global co-occurrence of high carbonate $\delta^{13}\text{C}$ values and enhanced siliceous plankton productivity (e.g., Bartolini *et al.*, 1996; Racki and Cordey, 2000; Morettini *et al.*, 2002; O'Dogherty *et al.*, 2006).

The plot of $\delta^{13}\text{C}$ versus $\delta^{18}\text{O}$ is used routinely to assess a potential diagenetic imprint on the stable-isotope record (e.g., Banner and Hanson, 1990; Huck *et al.*, 2013). A significant positive correlation between $\delta^{18}\text{O}$ and $\delta^{13}\text{C}$ may suggest a diagenetic imprint. This is because of a simultaneous decrease in both $\delta^{18}\text{O}$ and $\delta^{13}\text{C}$ values in rocks affected by meteoric or burial diagenesis (e.g., Banner and Hanson, 1990). Such plots for the values obtained reveal a weak correlation ($r^2 = 0.18, 0.06$ and 0.02 ; Fig. 14A). This suggests an insignificant influence of diagenetic alteration on the stable isotope records. Only the values from the Uplazińska Kopa section display moderate negative covariance ($r^2 = 0.36$).

Typical $\delta^{18}\text{O}$ values for Jurassic marine carbonates range between -3 and 0‰ (e.g., Jenkyns and Clayton, 1986). Diagenetic alteration generally leads to a decrease in the $\delta^{18}\text{O}$ values. The measured $\delta^{18}\text{O}$ values range from -6 to -1.4‰ . Although a 2‰ difference in $\delta^{18}\text{O}$ values of bulk carbonates was noted between the western and eastern parts of the Tatra Mountains, the shape of the $\delta^{13}\text{C}$ trends remains the same in both areas. This suggests that the carbon isotope composition of the sections studied is a reliable indicator of secular variations in the $\delta^{13}\text{C}$ values of marine carbonates.

The plot of $\delta^{13}\text{C}$ versus CaCO_3 shows a weak ($r^2 = 0.05$ and 0.02) or moderately (in the Western Tatra Mountains – $r^2 = 0.18$ and 0.23) negative covariance (Fig. 14B). Conversely, in the samples studied, a moderate positive covariance exists between $\delta^{18}\text{O}$ and CaCO_3 (Fig. 14C). Similarly, the pelagic deposits of the Terminilietto section (Umbria-Marche Basin) show lower $\delta^{18}\text{O}$ values in the presence of abundant cherts (Bartolini *et al.*, 1996). The authors suggested that such a negative shift may be diagenetic or palaeoenvironmental in origin (see discussion in Bartolini *et al.*, 1996).

Taking into account all of the aspects discussed above, it might be accepted that the $\delta^{13}\text{C}$ signal in the deposits studied is primary. Additionally, it suggests that $\delta^{13}\text{C}$ of bulk samples of micritic carbonates from carbonate-biosiliceous deposits, containing only a small amount of carbonate admixture (up to 12 wt% of CaCO_3), can be used effectively in chemostratigraphic studies.

Carbon-isotope stratigraphy

The unique $\delta^{13}\text{C}$ isotope pattern in the Middle–Upper Jurassic of the Tethyan region and the peri-Tethyan basins is relatively well recognized in bulk carbonate (e.g., Bartolini *et al.*, 1995, 1996, 1999; Weissert and Erba, 2004; O'Dogherty *et al.*, 2006; Louis-Schmid *et al.*, 2007) as well as in wood (e.g., Pearce *et al.*, 2005) and skeletal samples (e.g., Podlaha *et al.*, 1998; Wierzbowski, 2002, 2004). All these curves are characterized by distinctive shifts and pronounced trends, which are in most cases comparable (e.g., Pisera *et al.*, 1992; Gruszczynski, 1998; Jenkyns *et al.*, 2002; Brigaud *et al.*, 2009; Pellenard *et al.*, 2014). Interestingly, most carbon isotope trends for skeletal calcite are

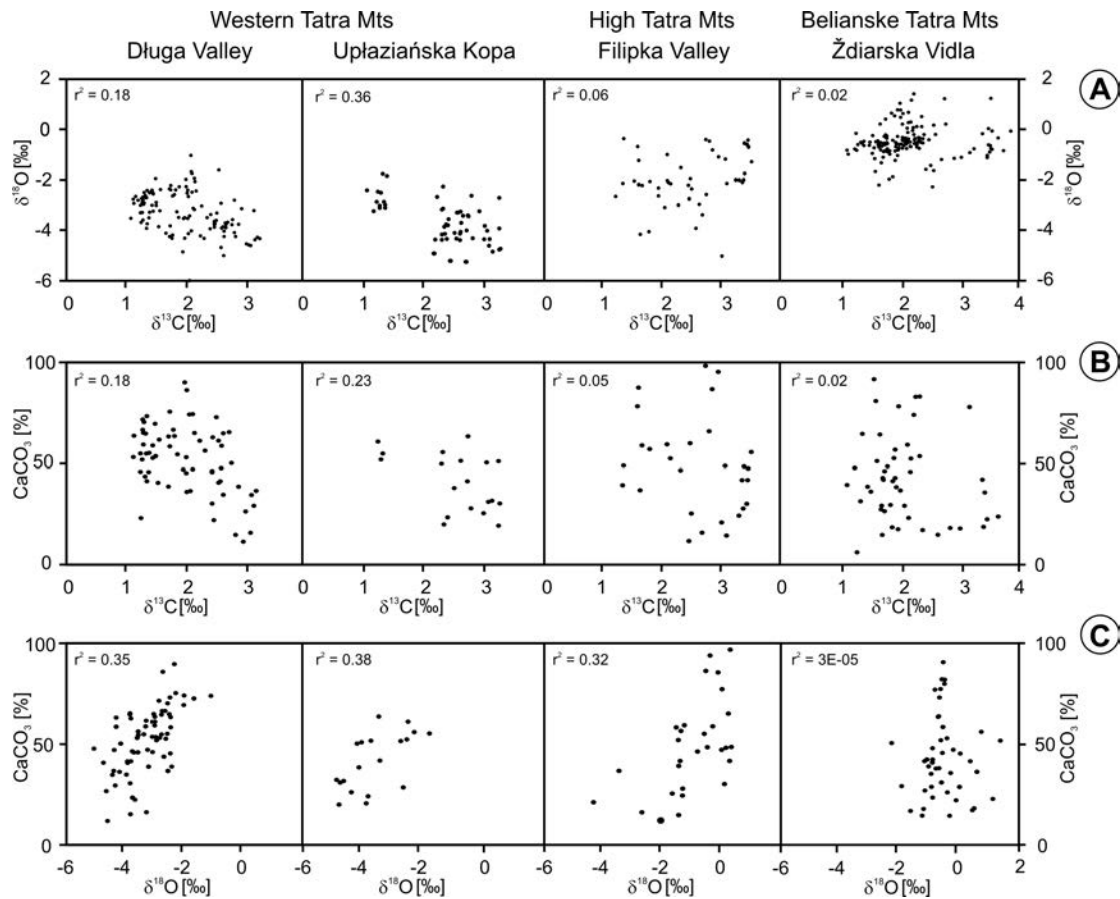


Fig. 14. Correlation of some geochemical parameters. **A.** Plot of $\delta^{13}\text{C}$ versus $\delta^{18}\text{O}$. The most negative $\delta^{18}\text{O}$ values occur in the Długa Valley and Uplazińska Kopa sections indicating that isotopic composition was slightly altered by burial diagenesis. **B.** $\delta^{13}\text{C}$ versus CaCO_3 content. The values show a moderate negative correlation or no covariance, indicating that silica diagenesis may not have influenced carbon isotopic signal. **C.** $\delta^{18}\text{O}$ versus CaCO_3 content. The values reveal a moderate positive correlation, indicating that silica had influence on the $\delta^{18}\text{O}$ record.

consistent with the trends in bulk carbonates, although absolute $\delta^{13}\text{C}$ values and amplitudes may differ. The bulk carbonate $\delta^{13}\text{C}$ curves are normally calibrated on the basis of ammonites (e.g., O'Dogherty *et al.*, 2006) or calcareous nannofossils (e.g., Bartolini *et al.*, 1995, 2003) and only rarely on radiolarians (Bartolini *et al.*, 1995). The data presented allow the establishment of a stratigraphic framework in, until now, poorly documented successions. The short-term and long-term isotope shifts and excursions identified were numbered from 1 to 8 (Fig. 15).

(1) The slight increase in $\delta^{13}\text{C}$ values (up to 2.5‰) is recorded in the interval 0–38 m in the spotted limestones and marls of the Ždiarska Vidla section (number 1 in Fig. 15). The age of these deposits is confirmed by ammonites, indicative of the Early Bajocian Propinquans Zone and the latest Bajocian and/or earliest Bathonian, described from the same facies in the Filipka Valley (Myczyński, 2004; Iwańczuk *et al.*, 2013). It is probable that $\delta^{13}\text{C}$ positive excursion (of 2.5‰), recorded in the lowermost part of the *Bositra*-crinoidal facies (0.5 m in the Długa Valley section), is the equivalent of the slight increase, noted above. However, the excursion cannot be identified unequivocally, owing to the lack of biostratigraphic data (Fig. 3). The limestones in question occur above the Toarcian–?Aalenian red

nodular limestones (Myczyński and Lefeld, 2003; Myczyński and Jach, 2009) and below the Upper Bathonian spotted radiolarites (data in this paper; see also Polák *et al.*, 1998). Hence both of the increases in $\delta^{13}\text{C}$ values from Ždiarska Vidla and Długa Valley sections are considered as a record of the Early Bajocian event (number 1 in Fig. 15).

The positive $\delta^{13}\text{C}$ excursion of Early Bajocian age was recorded in several sections of the Western Tethyan region, among others, from the Southern Alps (Zempolich and Erba, 1999; Baumgartner, 2013), Umbria-Marche Apennines (Fig. 16B; Bartolini *et al.*, 1996, 1999; Bartolini and Cecca, 1999; Morettini *et al.*, 2002), and the Betic Cordillera (Fig. 16F; O'Dogherty *et al.*, 2006), as well as from the French Subalpine Basin in the Digne region (Corbin, 1994 *vide* O'Dogherty *et al.*, 2006; Sucheras-Marx *et al.*, 2013). Radiolarian data from the Terminilto section in the Umbria-Marche Apennines permit reference of the excursion discussed to the UAZ 3 (Bartolini *et al.*, 1995; Fig. 16B). Detailed biostratigraphy, based on ammonites, dates precisely the range of this positive excursion as the Walkeri Subzone of the Discites Zone to the Romani Subzone of the Humphriesianum Zone (Fig. 16F; O'Dogherty *et al.*, 2006).

(2) The $\delta^{13}\text{C}$ curve in the interval 30–85 m of the Ždiarska Vidla section is difficult to interpret (Fig. 8),

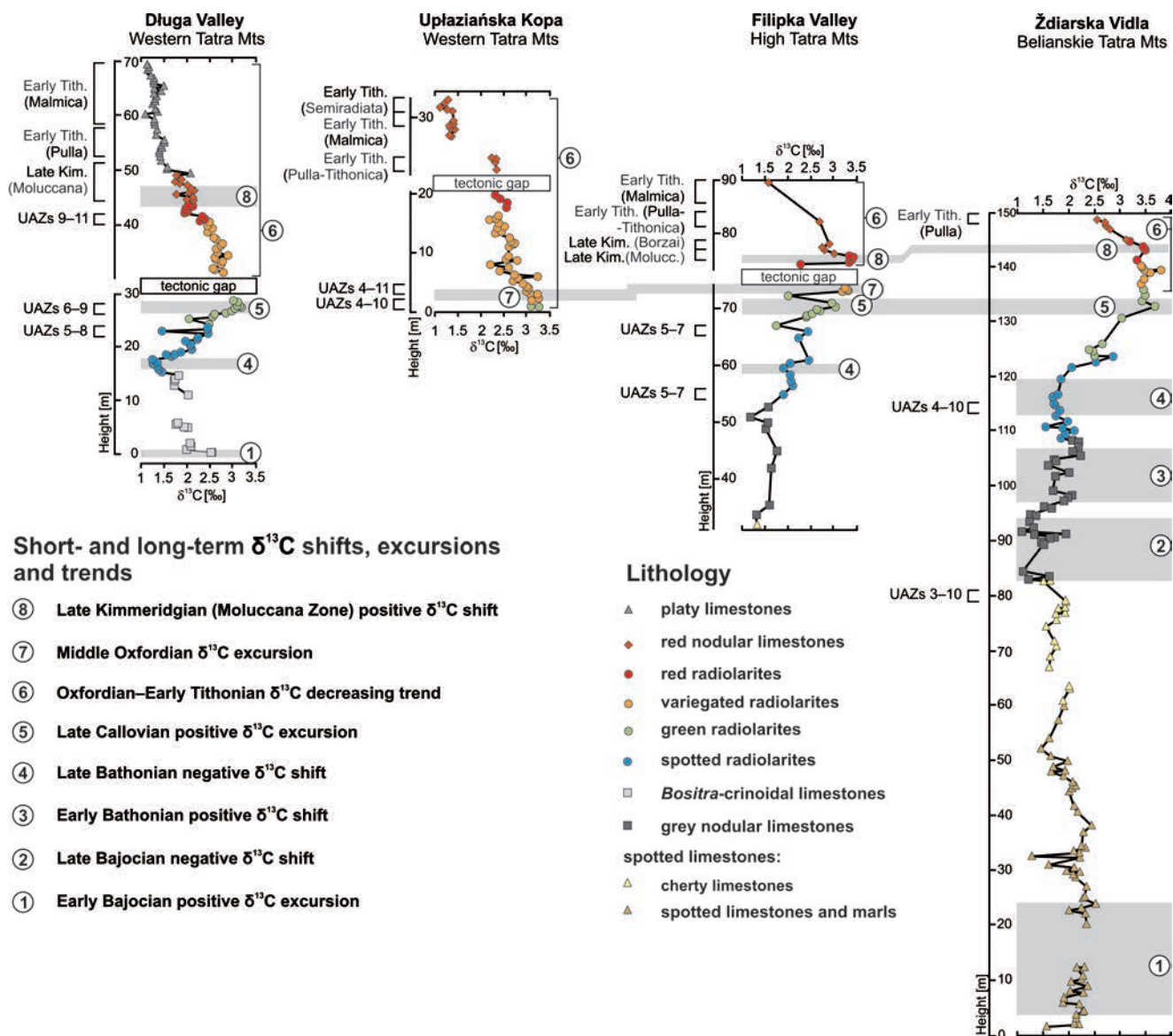


Fig. 15. Summary of correlation of the Bajocian–Early Tithonian $\delta^{13}\text{C}$ curves from the Krížna Unit of the Tatra Mountains.

mainly because of insufficient biostratigraphic data. In the interval 84–95 m of the lower part of the grey nodular limestones, the $\delta^{13}\text{C}$ values reach a minimum of about 1.1‰ (number 2 in Fig. 15). Such low values closely match the minimum of the carbon isotope curve from the Tethyan and peri-Tethyan regions, which corresponds to the latest Bajocian (Fig. 16A–C, F; e.g., Corbin, 1994 *vide* O'Dogherty *et al.*, 2006; Bartolini *et al.*, 1996, 1999; Gruszczynski, 1998; Jenkyns *et al.*, 2002; O'Dogherty *et al.*, 2006). The radiolarian data, presented in this paper, limit the upper range of the shift discussed to the Early Callovian (UAZs 5–7; Fig. 7), or more precisely to the Late Bathonian (Polák *et al.*, 1998). The Bajocian age of the shift seems to be contrary to the age of the underlying cherty limestones (Broniarski Limestone Member), which were dated by means of ammonites as the latest Bajocian and/or the earliest Bathonian in the Filipka Valley (Myczyński, 2004; Iwańczuk *et al.*, 2013). However, the ammonites were not precisely lo-

cated in the section. In fact, they could have come from the grey nodular limestones, which so far have not been distinguished in this section. Consequently, the latest Bajocian age is postulated for the $\delta^{13}\text{C}$ negative shift discussed (number 2 in Fig. 15).

(3) The minor positive $\delta^{13}\text{C}$ shift (of 2.2‰ and amplitude 0.9‰, number 3 in Fig. 15) in the interval 98–108 m in the Źdiarska Vidla section, may be correlated with the Early Bathonian event. It is supported only indirectly by sample Fp143, located in a similar position in the Filipka Valley section, which is just above grey nodular limestones (latest Bajocian to Early Callovian, UAZs 5–7; Fig. 7). The $\delta^{13}\text{C}$ shift was assigned to the Early Bathonian, on the basis of radiolarian correlation in the Umbria-Marche Apennines (Fig. 16B; Bartolini *et al.*, 1999) and ammonites in the Subbetic Basin (Fig. 16F; O'Dogherty *et al.*, 2006). Composite $\delta^{13}\text{C}$ curves, compiled by Gruszczynski (1998) and Jenkyns *et al.* (2002), also show the shift discussed (Fig. 16A, C).

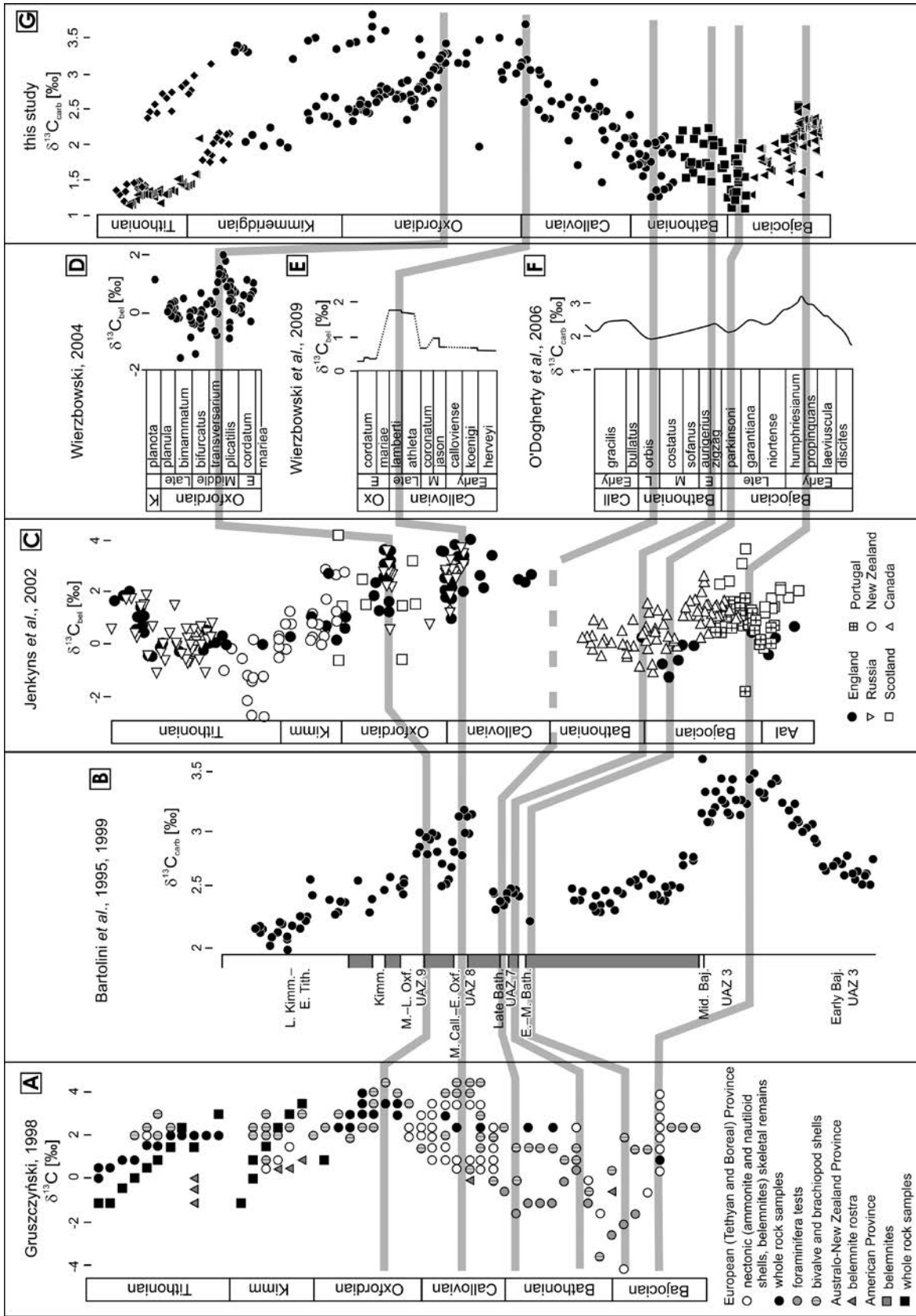


Fig. 16. Correlation of carbon-isotope data for the Middle-Late Jurassic. **A.** Composite data set (Gruszczyński, 1998). **B.** Pelagic carbonate deposits, Umbria Basin (Bartolini et al., 1995, 1999). **C.** Belemnites, Aalenian–Tithonian composite data set (Jenkyns et al., 2002), simplified. **D.** Belemnites, composite data set (Wierzbowski, 2004); Boreal-Subboreal belemnites from the Isle of Skye in Scotland are omitted. **E.** Belemnites, Polish Jura Chain (Wierzbowski et al., 2009). **F.** Hemipelagic carbonate deposits, Subbetic Basin (O'Dogherty et al., 2006). **G.** Pelagic biosiliceous-carbonate deposits, Krížna Nappe, Tatra Mts, this study.

(4) A negative $\delta^{13}\text{C}$ shift was identified in the lower part of the spotted radiolarites (number 4 in Fig. 15; in the Ždiarska Vidla section with a minimum of 1.7‰ at 116 m; in the Filipka Valley section with a minimum of 1.5‰ at 60 m, and in the Długa Valley section with a minimum of 1.2‰ at 18.5 m). Polák *et al.* (1998) dated this part of the sections at the Banie Huciska, Gładkie Uplaziańskie and Ždiarska Vidla as Late Bathonian–Early Callovian (UAZ 7, their samples HC-5, GU-2, GU-3, ŽV-8). New, less precise radiolarian data only prove its Late Bajocian–Early Callovian age (UAZs 5–7 in the samples Fp143, Fp269 in Fig. 7). A similar $\delta^{13}\text{C}$ shift, assigned to the Late Bathonian on the basis of radiolarian correlation (UAZ 7), was recorded in the Umbria-Marche Apennines (Fig. 16B; Bartolini *et al.*, 1995, 1996, 1999). In the Subbetic Basin, an analogous negative excursion has been recognized in the Upper Bathonian (Fig. 16F; O'Dogherty *et al.*, 2006). The same $\delta^{13}\text{C}$ pattern is evidenced from the composite data set, presented by Gruszczynski (1998; Fig. 16A). All these data suggest that the negative $\delta^{13}\text{C}$ shift discussed is referable to the Late Bathonian.

(5) The increasing trend in $\delta^{13}\text{C}$ values starts in the upper part of the Upper Bathonian–Lower Callovian spotted radiolarites (UAZ 7; Polák *et al.*, 1998; this study) and continues in the Middle Callovian–Lower Oxfordian green radiolarites (UAZ 8; Polák *et al.*, 1998; Banie Huciska, Gładkie Uplaziańskie, Ždiarska Vidla sections; their samples GU-6, HC-8, ŽV-2; this study, UAZs 6–9, sample Dsr96; Fig. 3). The sharp increase in $\delta^{13}\text{C}$ values results in a prominent positive excursion (number 5 in Fig. 15). It is documented in the uppermost part of the green radiolarites, in all of the curves presented, with the exception of the Uplaziańska Kopa section, and reaches an amplitude of 2%. In the Długa Valley section, the values exceed 3.2‰ at 29 m (Fig. 3) and in the Filipka Valley section 3‰ at 71 m (Fig. 7), whereas in the Ždiarska Vidla section the excursion reaches a value as high as 3.7‰ at the 133 m (Fig. 8). The new radiolarian data combined with the data presented by Polák *et al.* (1998) prove that the positive $\delta^{13}\text{C}$ excursion (number 5 in Fig. 15) can be taken as a record of the Late Callovian event.

The $\delta^{13}\text{C}$ curves presented show a remarkable similarity to the Callovian curves from several sections of the Western Tethyan and the peri-Tethyan basins. The $\delta^{13}\text{C}$ data of skeletal carbonate and bulk carbonate samples, presented by Gruszczynski (1998; Fig. 16A), show pronounced positive excursions in the Callovian. The same characteristic pattern is visible in the compilation, presented by Jenkyns *et al.* (2002; Fig. 16C). In the Southern Alps section in Italy, a clear positive excursion was recorded in the lower–middle part of the Callovian, followed by a minor positive peak for the Athleta Zone of the Upper Callovian (Jenkyns, 1996). Similar peaks were recognized in the pelagic deposits in the Umbria-Marche Apennines (Fig. 16B; Bartolini *et al.* 1995, 1996, 1999; Morettini *et al.*, 2002). Bartolini *et al.* (1995) proved that the pronounced positive excursion corresponds to the Middle Callovian–Early Oxfordian interval (UAZ 8). The observed pattern of the $\delta^{13}\text{C}$ curve from the sediments of the Tatra Mountains mirrors also the curve from the limestones of the western Sicily, which display

positive excursions in the Callovian (Cecca *et al.*, 2001). Interestingly, a similar $\delta^{13}\text{C}$ trend was recorded in the bivalve, belemnite and bulk carbonates from the Paris Basin. It shows slightly scattered, but increased $\delta^{13}\text{C}$ values in the Calloviense–Lamberti zones of the Callovian (Brigaud *et al.*, 2009). The age of this major Callovian positive $\delta^{13}\text{C}$ excursion in the Athleta and Lamberti zones (Upper Callovian), recorded in belemnite rostra from the Polish Jura Chain, is confirmed by precise ammonite stratigraphy (Wierzbowski *et al.*, 2009).

(6) Above the Late Callovian positive $\delta^{13}\text{C}$ excursion, the curves in all the sections show a steadily decreasing trend (number 6 in Fig. 15; UAZs 9–11 in sample Dsr191 in Figs 3, 6–8). It is comparable to the general pattern, recorded in several curves for the Western Tethyan region (Pisera *et al.*, 1992; Weissert and Mohr, 1996; Cecca *et al.*, 2001; Padden *et al.*, 2002; Weissert and Erba, 2004; Coimbra *et al.*, 2009). This decreasing trend is regarded as the most characteristic feature of the Late Jurassic $\delta^{13}\text{C}$ curves.

(7) In the decreasing trend, some $\delta^{13}\text{C}$ fluctuations are recorded. The most prominent of them are increases in $\delta^{13}\text{C}$ values, noted in the Uplaziańska Kopa section at 1.7 m (of 3.3‰, Fig. 6) and in the Filipka Valley section at 74 m (of 3.4‰, Fig. 7). In all these sections increased values occur in the lowermost part of the variegated radiolarites, which are dated as Middle–Late Oxfordian by means of radiolarian data (Polák *et al.*, 1998, UAZ 9 in the samples GU-10, GU-11). It is plausible that the shift mentioned above (number 7 in Fig. 15) reflects the Middle Oxfordian excursion, recorded in several $\delta^{13}\text{C}$ curves (e.g., Jenkyns, 1996; Weissert and Mohr, 1996; Bartolini *et al.*, 1995, 1999; Morettini *et al.*, 2002; Padden *et al.*, 2002; Rey and Delgado, 2002; Wierzbowski, 2002; Pearce *et al.*, 2005; Louis-Schmid *et al.*, 2007; Rais *et al.*, 2007; Coimbra *et al.*, 2009).

(8) The minor positive $\delta^{13}\text{C}$ shift (number 8 in Fig. 15), which culminates at 46 m in the Długa Valley section and at 76 m in the Filipka Valley section, was dated on the basis of calcareous dinoflagellates as in the Moluccana Zone of the Late Kimmeridgian (Figs 3, 7, 8). A similar shift, but without stratigraphic control, was recorded in the Ždiarska Vidla section at 142 m (Fig. 8). An analogue $\delta^{13}\text{C}$ shift was recognized in many Tethyan sections, for instance, in the Helvetic Nappes of eastern Switzerland and in the Southern Alps (Weissert and Mohr, 1996; Cecca *et al.*, 2001; Padden *et al.*, 2002). It was also identified in the Eudoxus Zone of the Late Kimmeridgian in the Kimmeridge Clay of Dorset of the north European basin (Fig. 16C; Morgans-Bell *et al.*, 2001; Jenkyns *et al.*, 2002). It is likely that the excursion discussed is correlated with a positive anomaly of the Late Kimmeridgian in the western Palaeo-Pacific region (Kakizaki and Kano, 2014).

Age of the studied deposits

Integrated radiolarian, calcareous dinoflagellate, calpionellid and stable isotope stratigraphy has shed new light on the age of the deposits studied and permits the establishment of a new stratigraphic scheme, which is presented and discussed below (Fig. 17).

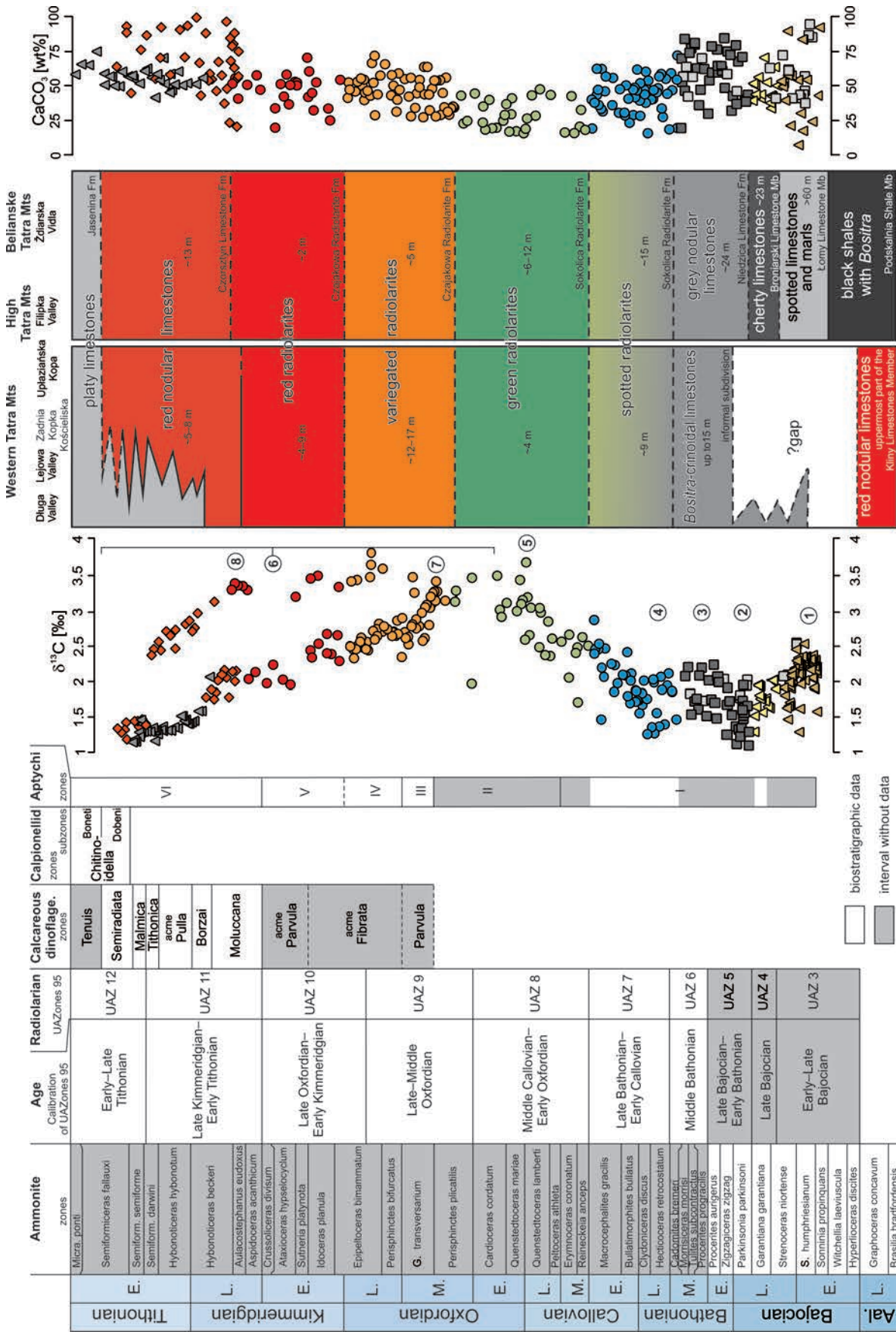


Fig. 17. Stratigraphic scheme of the Middle-Late Jurassic of the Krížna Nappe in the Tatra Mountains. Lithostratigraphic units after Lefeld *et al.* (1985) and Grabowski and Pszczółkowski (2006). Ammonite zonation and ages from Gradstein *et al.* (2004); radiolarian zonation by Baumgartner *et al.* (1995); calcareous dinoflagellate zonation by Reháková (2000); calpionellid zonation by Reháková (2002); aptychi zonation by Gaštorowski (1962); carbon isotope data and CaCO₃ content from this study.

Pre-radiolarite deposits

There is a great difference in the facies types of deposits, underlying the radiolarites between the Western Tatra Mountains and eastern part of the Tatras (the High Tatra and Belianske Tatra Mountains). In the former area the deposits were laid down on submarine highs, their slopes and in perched basins, whereas in the latter one a thick limestone-marl basinal succession was deposited (Iwanow, 1973; Lefeld, 1974; Wieczorek, 2001; Jach and Starzec, 2003; Gradziński *et al.*, 2004; Jach, 2005, 2007; Iwańczuk *et al.*, 2013). Facies changes have been noticed even over short distances, which indicate deposition in a basin with highly variable topography (Guzik, 1959; Jach, 2007).

The stratigraphy of the lower part of the Middle Jurassic deposits in the Western Tatra Mountains is poorly defined, which results from the scarcity of index fossils, incompleteness of the sections, as well as the common occurrence of condensations and hiatuses (Jach and Starzec, 2003; Gradziński *et al.*, 2004). The *Bositra*-crinoidal limestones studied overlie red nodular limestones, which in their middle part contain ammonites, diagnostic of the Serpentinum, Bifrons and Pseudoradosa zones of the Toarcian (Myczyński and Lefeld, 2003; Myczyński and Jach, 2009). The *Bositra*-crinoidal limestones are considered to be older than Late Bathonian, since the limestones discussed are directly followed by spotted radiolarites of the Late Bathonian–Early Callovian (see below; see also Polák *et al.*, 1998). Moreover, the recorded high $\delta^{13}\text{C}$ values probably refer to the Early Bajocian event (number 1 in Fig. 15) and are located below the Late Bathonian negative shift (number 4 in Fig. 15; Fig. 3).

Sedimentary features indirectly confirm the above view. The upper part of the underlying red nodular limestones, above the location of index ammonites, displays several characteristic features of condensed deposits, such as a concentration of microborings in bioclasts as well as the presence of ferruginous macroonoids, pelagic stromatolites and glauconite (Gradziński *et al.*, 2004). Thus, it points to a low rate of sedimentation. Moreover, the upper boundary of the red nodular limestones is an omission surface, which records a break in sedimentation and a stratigraphic hiatus (Jach, 2007). Similarly, concentration of glauconite grains and films indicates that the lower part of the *Bositra*-crinoidal limestones also represents condensed deposits.

The above view corresponds well with the broadly recorded phenomenon of non-deposition during the earliest Bajocian. It was recognized in several Tethyan sections (e.g., Morettini *et al.*, 2002; Gawlick *et al.*, 2009). The mass occurrence of *Bositra* at the top of the facies discussed also seems to be significant. The widespread occurrence of the *Bositra* microfacies is typical of the Bathonian and Callovian pelagic deposits of the Western Tethys and peri-Tethyan basins (e.g., Wierzbowski, 1994; Wierzbowski *et al.*, 1999; O'Dogherty *et al.*, 2006; Navarro *et al.*, 2009; Vörös, 2012). Collectively, all the above facts implicitly support the Bajocian–Bathonian age postulated for the limestones discussed.

In the deeper, basinal sections of the High Tatra and the Belianske Tatra Mountains, the Middle Jurassic interval includes spotted limestones with crinoidal turbidites (Mišík, 1959; Iwanow, 1973; Lefeld *et al.*, 1985). On the basis of the

ammonite assemblage, their age is regarded as Early Bajocian Propinquans Zone–latest Bajocian and/or earliest Bathonian (Myczyński, 2004; Iwańczuk *et al.*, 2013). An Early Bajocian age is also evidenced by the occurrence of the positive $\delta^{13}\text{C}$ excursion in the lower part of the spotted limestones and marls (number 1 in Fig. 15). The spotted limestones represent the basinal equivalent of the lowermost part of the *Bositra*-crinoidal limestones, which are related to a submarine highs (Fig. 17; see Iwańczuk *et al.*, 2013).

The grey nodular limestones, lying between the Bajocian spotted limestones and marls and younger radiolarites in the High Tatra and Belianske Tatra Mountains, were first described by Lefeld (1969). Radiolarian data (the latest Bajocian–Early Callovian, UAZs 5–7, sample Fp143) from overlying spotted radiolarites limit the upper boundary of the grey nodular limestones to the Early Callovian. Ammonites, indicative of the latest Bajocian and/or the earliest Bathonian, assigned by Myczyński (2004) and Iwańczuk *et al.* (2013) to the cherty limestones, most probably derive from the grey nodular limestones. Carbon isotope analysis provided additional information on their age. The $\delta^{13}\text{C}$ curve in the grey nodular limestones shows negative and positive shifts (number 2 and 3 in Fig. 15; the Ždiarska Vidla section), which probably are referable to the latest Bajocian and the Early Bathonian. Thus, the grey nodular limestones with abundant *Bositra* shells are the basinal equivalent of the upper part of the *Bositra*-crinoidal limestones.

Age of radiolarites

The lowermost radiolarites were assigned by Polák *et al.* (1998) to the Late Bathonian–Early Callovian (UAZ 7; Banie Huciska and Gładkie Uplaziańskie sections). A Middle Bathonian age was also implied for the lowermost part of the Sokolica Radiolarite Formation in the Filipka Valley (Bał, 2001).

The newly analysed radiolarians only confirmed that the lowermost part of the spotted radiolarites may be assigned to the Upper Bajocian–Lower Callovian (UAZs 5–7). Additionally, carbon isotope analyses permit the determination of the Late Bathonian negative $\delta^{13}\text{C}$ shift in their lower part (number 4 in Fig. 15). Only one *Lamellaptychus* sp. was found in the spotted radiolarites in the Grześ section in the Western Tatra Mountains, indicating that they are not older than Bajocian (Gašiorowski, 1959, 1962). Thus, the spotted radiolarites are of Late Bathonian–Early Callovian age, although a Middle Bathonian age cannot be excluded.

The age of the green radiolarites is estimated to span from the Middle Callovian to the Early Oxfordian on the basis of radiolarians (UAZ 8; Polák *et al.*, 1998). The pronounced positive $\delta^{13}\text{C}$ excursion (number 5 in Fig. 15), identified as Late Callovian and detected in the uppermost part of green radiolarites, additionally confirm their age. It is worth mentioning that this excursion coincides with a distinct increase in radiolarian abundance and an extreme carbonate production crisis (Bartolini *et al.*, 1999; Morettini *et al.*, 2002).

A radiolarian assemblage indicative of the Middle Oxfordian–Early Kimmeridgian (UAZs 9–10) was determined in the variegated radiolarites (this study; Polák *et al.*, 1998). The boundary between the variegated and red radiolarites cannot be dated precisely. Hence, the variegated radiolarites

can be assigned to the Middle Oxfordian–Late Oxfordian or Early Kimmeridgian.

The red radiolarites represent the latest Oxfordian or Early Kimmeridgian–earliest Late Kimmeridgian (Jach *et al.*, 2012; and this study). The radiolarian assemblage corresponds to the wide interval, ranging from the Middle–Late Oxfordian to the Early Tithonian (UAZs 9–11), whereas calcareous dinoflagellates from the upper part of the red radiolarites limit their upper range to the Moluccana Zone of the Late Kimmeridgian (Jach *et al.*, 2012). This is in line with the opinion of Gařiorowski (1959, 1962), who assigned the red radiolarites to the Late Oxfordian–Early Kimmeridgian (IV and V aptychi horizons *sensu* Gařiorowski, 1962; Fig. 17). The positive $\delta^{13}\text{C}$ shift (number 8 in Fig. 15) in the upper part of the red radiolarites in the Filipka Valley and Źdiarska Vidla sections (Figs 6, 7) is dated precisely by means of calcareous dinoflagellates as belonging to the Moluccana Zone of the Late Kimmeridgian.

Post-radiolarite deposits

Calcareous dinoflagellates and carbon isotope data (number 8 in Fig. 15) allow estimation of the onset of sedimentation of the red nodular limestones as referable to the Moluccana Zone of the Late Kimmeridgian (Długa Valley, Fig. 3). Interestingly, the same excursion in the Filipka Valley section and probably also in the Źdiarska Vidla section was detected in the red radiolarites (Figs 7, 8). The difference may be explained either by facies diachroneity or by the fact that a part of the curve is missing, owing to erosion or a non-deposition hiatus, at which a part of the Moluccana Zone is absent. Breccias identified in the lowermost part of the red nodular limestones at the Źdiarska Vidla section tend to confirm the latter possibility.

The red nodular limestones have a diachronous upper boundary, which ranges from the Moluccana Zone of the Late Kimmeridgian to the Malmica Zone of the Early Tithonian (see Jach *et al.*, 2012). In the Długa Valley and Lejowa Valley sections, they interfinger with platy limestones. These new stratigraphic data correspond well with the aptychi data presented by Gařiorowski (1959, 1962) from the Grzeř section in the Western Tatra Mountains. The aptychi assemblage, dominated by Lamellaptychi from group A, is indicative of the Late Kimmeridgian–Early Tithonian (horizon VI₁ *sensu* Gařiorowski, 1962). The Late Kimmeridgian–Early Tithonian age of the red nodular limestones is also confirmed by the abundant occurrence of the *Saccocoma* and *Globochaete* microfacies (Borza, 1984; Wierzbowski, 1994; Reháková, 2000).

In the sections studied, platy limestones range up to the calpionellid Boneti Subzone (Chitinoidella Zone) of the latest Early Tithonian. The abundant occurrence of *Saccocoma* and *Globuligerina* confirms their Late Kimmeridgian (Moluccana and Borzai zones)–Early Tithonian age (Pulla–Malmica zones; Grabowski and Pszczółkowski, 2006; Jach *et al.*, 2012; Grabowski *et al.*, 2013).

Regional distribution and age of radiolarites

The data presented above on the basis of integrated biostratigraphy and isotope stratigraphy permit the sedimenta-

tion of radiolarites in the Tatra Mountains to be seen as limited to the Late Bathonian–early Late Kimmeridgian. The above view also is generally consistent with the previous opinion on the age of radiolarites in other parts of the Krížna Nappe (Miřík, 1999). Radiolarites in several successions of the Krížna Nappe (for correlations see Fig. 18) range from the Late Bathonian or from the Late Callovian to the Early Kimmeridgian (UAZs 7 or 8–10; Polák and Ondrejčková, 1993). Similarly, radiolarites of the Šipruň succession of the Tatricum Domain range from the Late Bathonian to the Early Kimmeridgian (UAZs 8–10; Polák and Ondrejčková, 1995). However, in the Krížna Nappe of the Tatra Mountains, some radiolarian-bearing limestones or thin radiolarite intercalations were laid down as early as in the Bajocian (Figs 7, 17, 18; see also Iwańczuk *et al.*, 2013). By analogy, in the Manín Unit, which is considered to be the northern part of the Fatricum Domain (Plařienka, 2012), radiolarites 2.5 m thick and sandwiched between red nodular limestones were dated as Late Bathonian (Rakús and Ořvoldová, 1999).

In addition to the Fatricum, Manín and Tatricum domains, radiolarites were deposited in other domains of the Western Carpathians (Miřík, 1999). In the Meliaticum Domain, which was a remnant of the former ocean existing in Triassic and Jurassic times, the radiolarites were dated at the Ladinian–Norian, and Middle Bathonian–Early Oxfordian (Havřila and Ořvoldová, 1996; Kozur and Mock, 1996; Kozur *et al.*, 1996; Mock *et al.*, 1998). The Meliata Domain was the only one unit developed on an oceanic crust.

The Silicicum Domain, the palaeogeographic location of which is controversial, is the southernmost of them. It could have been situated on the southern or northern margin of the Meliata Ocean (Plařienka, 1998; Csontos and Vörös, 2004). In the Silicicum Domain, radiolarite sedimentation persisted from the Late Bathonian to the Oxfordian (Sýkora and Ořvoldová, 1996). However, the oldest known Jurassic radiolarian assemblage in this domain is of latest Bajocian–Early Bathonian age (UAZ 5; Ořvoldová, 1997, 1998). Similarly, in the Hronicum Domain, the palaeogeographic position of which is slightly enigmatic, the onset of radiolarite sedimentation took place between the Middle Bathonian and the Early Callovian (Polák and Ořvoldová, 2001).

The Belice Unit of the Povařský Inovec Mountains represents the exposure of deposits assigned to the Vahicum Domain. Radiolarites from this succession were dated as the lower part of the Early Oxfordian to the Kimmeridgian or even the Tithonian (UAZs 8–10; Ořvoldová, 1990; Plařienka, 2012). Similarly, in the deeper-water successions (e.g., Pieniny, Branisko and Kysuca successions) of the Pieniny Klippen Belt, which is a more northerly domain in the Central Carpathians, continuous radiolarite sedimentation persisted from the Middle Callovian to the Early Kimmeridgian (UAZs 8–10; Birkenmajer, 1977; Widz, 1991; Ořvoldová, 1992; Miřík *et al.*, 1994; Birkenmajer and Widz, 1995; Plařienka and Ořvoldová, 1996; Ořvoldová and Frantová, 1997; Ořvoldová *et al.*, 2000). However, some radiolarite interbeds within the red nodular limestones of the Kysuca succession and within the dark, spotted siliceous limestones and marls (Podzamcze Formation, Upper *Posidonia* Beds in the older nomenclature) of the Pieniny succession, contain

flected synsedimentary tectonic activity (e.g., Bernoulli and Jenkyns, 1974). Thus, the differences in age between the above domains and the Pieniny Klippen Belt, located to the north of them (in the present coordinates) may have resulted from different subsidence rates in these regions.

The Fatricum Domain of the Central Western Carpathians is considered to be a lateral equivalent of the Middle Austroalpine units of the Eastern Alps (e.g., Mišík *et al.*, 1991; Häusler *et al.*, 1993; Csontos and Vörös, 2004). Although the Jurassic palaeogeographic position of the Central Carpathian and Eastern Alpine domains is well documented, their precise correlation may be complicated (e.g., Häusler *et al.*, 1993; Kozur and Mock, 1996). The Jurassic succession of the Fatricum Domain (Křížna Nappe) reveals many analogies to the Bajuvaricum units of the Northern Calcareous Alps (see also Plašienka, 1998). This unit is regarded as the equivalent of the Hronicum Domain, based mainly on Triassic facies. However, its Jurassic facies development shows some striking similarities to the Fatricum Domain (Froitzheim *et al.*, 2008; Gawlick *et al.*, 2009). The similarities relate also to the age of the radiolarites. Cherty limestones of the Chiemgau series, which are lithologically similar to the Tatra spotted radiolarites, for the most part are of Bathonian–Callovian age. The overlying Ruhpolding Formation, which seems to be the age and lithological equivalent of the green, variegated and red radiolarites, was laid down in the Callovian to the Kimmeridgian (Gawlick *et al.*, 2009).

CONCLUSIONS

1. Radiolarian, calcareous dinoflagellate and calpionellid data, combined with the carbon isotope record, permit correlation of the Bajocian–Lower Tithonian pelagic deposits of the Křížna Nappe in the Tatra Mountains (Carpathians, Poland and Slovakia) and estimation of the stratigraphic range of the facies distinguished.

2. Carbon isotope curves show positive excursions and shifts in the Early Bajocian, Early Bathonian, Late Callovian, Middle Oxfordian and Late Kimmeridgian (Moluccana Zone) and negative ones in the latest Bajocian and Late Bathonian. The most prominent excursion of the Late Callovian is recorded in highly siliceous green radiolarites, which are strongly depleted in CaCO₃.

3. The Middle Jurassic pre-radiolarite deposits show distinct facies changes. A basin succession is represented by Bajocian spotted limestones, which are succeeded by uppermost Bajocian–Middle Bathonian grey nodular limestones. Simultaneously, condensed *Bositra*-crinoidal limestones were laid down on submarine highs and their slopes.

4. Uniform radiolarite sedimentation started in the Late Bathonian or somewhat earlier in the latest Middle Bathonian, but intermittent sedimentation of radiolarian-bearing deposits is documented in the Late Bajocian. This kind of sedimentation persisted to the early Late Kimmeridgian.

5. A return to carbonate sedimentation took place in the Late Kimmeridgian (Moluccana Zone), when red nodular limestones were deposited.

6. Carbon stratigraphy is a reliable tool for the correla-

tion of pelagic biosiliceous-carbonate successions, as was the case for the pelagic carbonate successions that were extensively studied up to now.

Acknowledgments

We gratefully acknowledge Ladislava Ožvoldová for her help and advice regarding Carpathian radiolarites. Special thanks go to Michał Gradziński, Mariusz Mucha and Alfred Uchman for excellent field assistance. Renata Jach and Nevenka Djerić were financed by Grant N N307 016537. The work of Daniela Reháková was supported by the Grant Agency of the Slovak Republic VEGA 2/0068/11, VEGA 2/0042/12 and LPP 0120-09. The work of Nevenka Djerić and Špela Goričan was partly supported by the Ministry of Education, Science and Technological Development of the Republic of Serbia (Project No. 176015) and the Slovenian Research Agency (Project No. P1-0008), respectively. The authorities of the Polish Tatra National Park (TPN, Zakopane) and the Slovak Tatra National Park (TANAP, Tatranská Lomnica) provided permission for the fieldwork, for which the authors are very grateful. The authors also warmly acknowledge Ewa Malata for her help and constructive comments on the paper. Reviews by Daria Ivanova, José Sandoval, Hisashi Suzuki and Hubert Wierzbowski, and editorial work by Alfred Uchman and Frank Simpson greatly improved the paper. Hisashi Suzuki is acknowledged for comments on the taxonomy of radiolarians, although not all of these suggestions were implemented.

REFERENCES

- Aubrecht, R. & Ožvoldová, L., 1994. Middle Jurassic – Lower Cretaceous development of the Pruské Unit in the western part the Pieniny Klippen Belt. *Geologica Carpathica*, 45: 211–223.
- Bac-Moszaszwili, M., Burchart, J., Głazek, J., Iwanow, A., Jaroszewski, W., Kotański, Z., Lefeld, J., Mastella, L., Ozimkowski, W., Roniewicz, P., Skupiński, A. & Westwalewicz-Mogilska, E., 1979. *Geological Map of the Polish Tatra Mountains 1:30 000*. Wydawnictwa Geologiczne, Warszawa.
- Banner, J. & Hanson, G. N., 1990. Calculation of simultaneous isotopic and trace element variations during water-rock interaction with applications to carbonate diagenesis. *Geochimica et Cosmochimica Acta*, 54: 3123–3137.
- Bartolini, A., Baumgartner, P. O. & Guex, J., 1999. Middle and Late Jurassic radiolarian palaeoecology versus carbon-isotope stratigraphy. *Palaeogeography, Palaeoclimatology, Palaeoecology*, 145: 43–60.
- Bartolini, A., Baumgartner, P. O. & Hunziker, J., 1996. Middle and Upper Jurassic carbon stable-isotope stratigraphy and radiolarites sedimentation of the Umbria-Marche basin (Central Italy). *Eclogae Geologicae Helvetiae*, 89: 811–844.
- Bartolini, A., Baumgartner, P. O. & Mattioli, E., 1995. Middle and Late Jurassic radiolarian biostratigraphy of the Colle Bertone and Terminetto sections (Umbria–Marche–Sabina Apennines, Central Italy): an integrated stratigraphy approach. In: Baumgartner, P. O., O'Dogherty, L., Goričan, Š., Urquhart, E., Pillevert, A. & De Wever, P. (eds), *Middle Jurassic to Lower Cretaceous Radiolaria of Tethys: Occurrences, Systematics, Biochronology*. *Mémoires de Géologie, Lausanne*, 23: 817–831.
- Bartolini, A. & Cecca, F., 1999. 20 My hiatus in the Jurassic of Umbria-Marche Apennines (Italy): carbonate crisis due to eutrophication. *Comptes Rendus de l'Académie des Sciences*.

- Série 2, Sciences de la Terre et des Planètes*, 329: 587–595.
- Bartolini, A., Pittet, B., Mattioli, E. & Hunziker, J. C., 2003. Regional control on stable isotope signature in deep-shelf sediments: an example of the Late Jurassic of southern Germany (Oxfordian–Kimmeridgian). *Sedimentary Geology*, 160: 107–130.
- Baumgartner, P. O., 1987. Age and genesis of Tethyan Jurassic radiolarites. *Eclogae Geologicae Helvetiae*, 80: 831–879.
- Baumgartner, P. O., 2013. Mesozoic radiolarites – Accumulation as a function of sea surface fertility on Tethyan margins and in ocean basins. *Sedimentology*, 60: 292–318.
- Baumgartner, P. O., Bartolini, A., Carter, E. S., Conti, M., Cortese, G., Danelian, T., De Wever, P., Dumitrica, P., Dumitrica-Jud, R., Goričan, Š., Guex, J., Hull, D. M., Kito, N., Marcucci, M., Matsuoka, A., Murchey, B., O'Dogherty, L., Savary, J., Vishnevskaya, V., Widz, D., Yao, A., 1995. Middle Jurassic to Early Cretaceous radiolarian biochronology of Tethys based on Unitary Associations. In: Baumgartner, P. O., O'Dogherty, L., Goričan, Š., Urquhart, E., Pillecuit, A. & De Wever, P. (eds), *Middle Jurassic to Lower Cretaceous Radiolaria of Tethys: Occurrences, Systematics, Biochronology*. *Mémoires de Géologie, Lausanne*, 23: 1013–1038.
- Bąk, M., 2001. Promienice z kompleksu radiolarytów środkowej i górnej jury jednostki reglowej dolnej Tatr – ich znaczenie biostratygraficzne. In: Bąk, K. (ed.), *Przewodnik Sympozjum Terenowego, III Ogólnopolskie Warsztaty Mikropaleontologiczne, Zakopane 2001*. Akademia Pedagogiczna w Krakowie, Kraków, pp. 50–53. [In Polish].
- Bernoulli, D. & Jenkyns, H. C., 1974. Alpine, Mediterranean and Central Atlantic Mesozoic facies in relation to the early evolution of the Tethys. In: Dott, R. H. & Sharer, R. H. (eds), *Modern and Ancient Geosynclinal Sedimentation*. *Society of Economic Paleontologists and Mineralogists, Special Publication*, 19: 129–160.
- Bill, M., O'Dogherty, L., Guex, J., Baumgartner, P. O. & Masson, H., 2001. Radiolarite ages in Alpine-Mediterranean ophiolites: constraints on the oceanic spreading and the Tethys-Atlantic connection. *Bulletin of the Geological Society of America*, 113: 129–143.
- Birkenmajer, K., 1977. Jurassic and Cretaceous lithostratigraphy units of the Pieniny Klippen Belt, Carpathians, Poland. *Studia Geologica Polonica*, 45: 1–158.
- Birkenmajer, K. & Widz, D., 1995. Biostratigraphy of Upper Jurassic radiolarites in the Pieniny Klippen Belt, Carpathians. In: Baumgartner, P. O., O'Dogherty, L., Goričan, Š., Urquhart, E., Pillecuit, A. & De Wever, P. (eds), *Middle Jurassic to Lower Cretaceous Radiolaria of Tethys: Occurrences, Systematics, Biochronology*. *Mémoires de Géologie, Lausanne*, 23: 889–896.
- Bojanowski, M. J., Barczuk, A. & Wetzel, A., 2014. Deep-burial alteration of early diagenetic carbonate concretions formed in Palaeozoic deep-marine greywackes and mudstones (Bardo Unit, Sudetes Mountains, Poland). *Sedimentology*, DOI: 10.1111/sed.12098
- Borza, K., 1984. The Upper Jurassic–Lower Cretaceous parabiostrophic scale on the basis of Tintinninae, Cadosinidae, Stomiosphaeridae, Calcisphaerulidae and other microfossils from the West Carpathians. *Geologický Zborník – Geologica Carpathica*, 35: 539–550.
- Borza, K. & Michalík, J., 1986. Problems with delimitation of the Jurassic/Cretaceous boundary in the Western Carpathians. *Acta Geologica Hungarica*, 29: 133–149.
- Brigaud, B., Durlet, C., Deconinck, J.-F., Vincent, B., Pucéat, E., Thierry, J. & Trouiller, A., 2009. Facies and climate/environmental changes recorded on a carbonate ramp: a sedimentological and geochemical approach on Middle Jurassic carbonates (Paris Basin, France). *Sedimentary Geology*, 222: 181–206.
- Cecca, F., Savary, B., Bartolini, A., Remane, J. & Cordey, F., 2001. The Middle Jurassic–Lower Cretaceous Rosso Ammonitico succession of Monte Inici (Trapanese domain, western Sicily): sedimentology, biostratigraphy and isotope stratigraphy. *Bulletin de la Société Géologique de France*, 172: 647–659.
- Coimbra, R., Immenhauser, A. & Olóriz, F., 2009. Matrix micrite $\delta^{13}\text{C}$ and $\delta^{18}\text{O}$ reveals synsedimentary marine lithification in Upper Jurassic Ammonitico Rosso limestones (Betic Cordillera, SE Spain). *Sedimentary Geology*, 219: 332–348.
- Colombié, C., Lécuyer, C. & Strasser, A., 2011. Carbon- and oxygen-isotope records of palaeoenvironmental and carbonate production changes in shallow-marine carbonates (Kimmeridgian, Swiss Jura). *Geological Magazine*, 148: 133–153.
- Corbin, J. C., 1994. *Evolution géochimique du Jurassique du Sud-est de la France: influence des variations du niveau marin et de la tectonique*. Unpublished PhD Thesis, Paris VI University, 175 pp.
- Csontos, L. & Vörös, A., 2004. Mesozoic plate tectonic reconstruction of the Carpathian region. *Palaeogeography, Palaeoclimatology, Palaeoecology*, 210: 1–56.
- Dunham, R. J., 1962. Classification of carbonate rocks according to depositional texture. In: Ham, W. E. (ed.), *Classification of Carbonate Rocks. A Symposium*. *American Association of Petroleum Geologists, Memoire*, 1: 108–121.
- Froitzheim, N., Plašienka, D. & Schuster, R., 2008. Alpine tectonics of the Alps and Western Carpathians. In: McCann, T. (ed.), *The Geology of Central Europe, Volume 2: Mesozoic and Cenozoic*. Geological Society, London, pp. 1141–1232.
- Gawlick, H.-J., Missoni, S., Schagintweit, F., Suzuki, H., Frisch, W., Krystyn, L., Blau, J. & Lein, R., 2009. Jurassic tectonostratigraphy of Austroalpine domain. *Journal of Alpine Geology*, 50: 1–152.
- Gąsiorowski, S. M., 1959. On the age of radiolarites in the Sub-Tatric series in the Tatra Mts. *Acta Geologica Polonica*, 9: 221–230. [In Polish, English summary].
- Gąsiorowski, S. M., 1962. Aptychi from the Dogger, Malm and Neocomian in the Western Carpathians and their stratigraphical value. *Studia Geologica Polonica*, 10: 1–151.
- Grabowski, J. & Pszczółkowski, A., 2006. Magneto- and biostratigraphy of the Tithonian–Berriasian pelagic sediments in the Tatra Mountains (central Western Carpathians, Poland): sedimentary and rock magnetic changes at the Jurassic/Cretaceous boundary. *Cretaceous Research*, 27: 398–417.
- Grabowski, J., Schnyder, J., Sobieñ, K., Koptiková, L., Krzemiński, L., Pszczółkowski, A., Hejnar, J. & Schnabl, P., 2013. Magnetic susceptibility and spectral gamma logs in the Tithonian–Berriasian pelagic carbonates in the Tatra Mts (Western Carpathians, Poland): palaeoenvironmental changes at the Jurassic/Cretaceous boundary. *Cretaceous Research*, 43: 1–17.
- Gradstein, F., Ogg, J. & Smith, A., 2004. *A Geologic Time Scale 2004*. Cambridge: Cambridge University Press, 589 pp.
- Gradziński, M., Tyszka, J., Uchman, A. & Jach, R., 2004. Large microbial-foraminiferal ooids from condensed Lower-Middle Jurassic deposits: A case study from the Tatra Mountains, Poland. *Palaeogeography, Palaeoclimatology, Palaeoecology*, 213: 133–151.
- Gruszczyński, M., 1998. Chemistry of Jurassic seas and its bearing on the existing organic life. *Acta Geologica Polonica*, 48: 1–29.
- Guzik, K., 1959. Notes on some stratigraphic problems of the Lias–Dogger rocks in the Lower Sub-Tatric Nappe of the

- Tatra Mountains. *Biuletyn Geologiczny*, 149: 183–188. [In Polish, English summary].
- Havrila, M., & Ožvoldová, L., 1996. Meliaticum in the Stratenská hornatina Hills. *Slovak Geological Magazine*, 96: 335–339.
- Häusler, H., Plašienka, D. & Polák, M., 1993. Comparison of Mesozoic successions in the Central Eastern Alps and the Central Western Carpathians. *Jahrbuch der Geologischen Bundesanstalt*, 136: 715–739.
- Huck, S., Heimhofer, U., Immenhauser, A. & Weissert, H., 2013. Carbon-isotope stratigraphy of Early Cretaceous (Urgonian) shoal-water deposits: Diachronous changes in carbonate-platform production in the north-western Tethys. *Sedimentary Geology*, 290: 157–174.
- Iwanow, A., 1973. New data on geology of the Lower Subtatic Succession in the eastern part of the Tatra Mts. *Bulletin of the Polish Academy of Sciences, Earth Sciences*, 21: 65–74.
- Iwańczuk, J., Iwanow, A. & Wierzbowski, A., 2013. Lower Jurassic to lower Middle Jurassic succession at Kopy Sołtysie and Placziwa Skała in the eastern Tatra Mts (Western Carpathians) of Poland and Slovakia: stratigraphy, facies and ammonites. *Volumina Jurassica*, 11: 19–58.
- Jach, R., 2002. Lower Jurassic spiculite series from the Krížna Unit in the Tatra Mts, Western Carpathians, Poland. *Annales Societatis Geologorum Poloniae*, 72: 131–144.
- Jach, R., 2005. Storm-dominated deposition of the Lower Jurassic crinoidal limestones in the Krížna Unit, Western Tatra Mountains, Poland. *Facies*, 50: 561–572.
- Jach, R., 2007. *Bositra* limestones – a step towards radiolarites: case study from the Tatra Mountains. *Annales Societatis Geologorum Poloniae*, 77: 161–170.
- Jach, R., Reháková, D. & Uchman, A., 2012. Biostratigraphy and palaeoenvironment of the Kimmeridgian–Lower Tithonian pelagic sediments of the Krížna Nappe, Lejowa Valley, Tatra Mts., southern Poland. *Geological Quarterly*, 56: 773–788.
- Jach, R. & Starzec, K., 2003. Glaucony from the condensed Lower-Middle Jurassic deposits of the Krížna Unit, Western Tatra Mountains, Poland. *Annales Societatis Geologorum Poloniae*, 73: 183–192.
- Jarvis, I., Mabrouk, A., Moody, R. T. J. & de Cabrera, S., 2002. Late Cretaceous (Campanian) carbon isotope events, sea-level change and correlation of the Tethyan and Boreal realms. *Palaeogeography, Palaeoclimatology, Palaeoecology*, 188: 215–248.
- Jenkyns, H. C., 1996. Relative sea-level change and carbon isotopes; data from the Upper Jurassic (Oxfordian) of central and southern Europe. *Terra Nova*, 8: 75–85.
- Jenkyns, H. C. & Clayton, C. J., 1986. Black shales and carbon isotopes in pelagic sediments from the Tethyan Lower Jurassic. *Sedimentology*, 33: 87–106.
- Jenkyns, H. C., Jones, C., Gröcke, D. R., Hesselbo, S. P. & Parkinson, D. N., 2002. Chemostratigraphy of the Jurassic System: applications, limitations and implications for palaeoceanography. *Journal of the Geological Society*, 159: 351–378.
- Kakizaki, Y. & Kano, A., 2014. Carbon isotope stratigraphy of Torinosu-type limestones in the western Paleo-Pacific and its implication to paleoceanography in the Late Jurassic and earliest Cretaceous. *Island Arc*, 23: 16–32.
- Kozur, H. & Mock, R., 1996. New palaeogeographic and tectonic interpretations in the Slovakian Carpathians and their implications for correlations with the Eastern Alps. Part I: Central Western Carpathians. *Mineralia Slovaca*, 28: 151–174.
- Kozur, H., Mock, R. & Ožvoldová, L., 1996. New biostratigraphic results in the Meliaticum in its type area around Meliata village (Slovakia) and their tectonic and paleogeographic significance. *Geologische Paläontologische Mitteilungen Innsbruck*, 21: 89–121.
- Lakova, I., Stoykova, K. & Ivanova, D., 1999. Calpionellid, nannofossils, and calcareous dinocyst bioevents and integrated biochronology of the Tithonian to Valanginian in the West Balcan Mountains, Bulgaria. *Geologica Carpathica*, 50: 151–168.
- Lefeld, J., 1969. Upper Jurassic carbo-silite sequence in the Sub-Tatric Succession of the Eastern Tatra Mts. *Bulletin of the Polish Academy of Sciences, Earth Sciences*, 17: 29–35.
- Lefeld, J., 1974. Middle-Upper Jurassic and Lower Cretaceous biostratigraphy and sedimentology of the Sub-Tatric Succession in the Tatra Mts. (Western Carpathians). *Acta Geologica Polonica*, 24: 277–364.
- Lefeld, J., 1981. Upper Jurassic radiolarite – nodular limestone vertical symmetry in the Polish Central Carpathians as reflection of regional depth changes in the ocean. *Studia Geologica Polonica*, 68: 89–96.
- Lefeld, J., Gaździcki, A., Iwanow, A., Krajewski, K. & Wójcik, K., 1985. Jurassic and Cretaceous lithostratigraphic units in the Tatra Mts. *Studia Geologica Polonica*, 84: 7–93.
- Louis-Schmid, B., Rais, P., Schaeffer, P., Bernasconi, S. & Weissert, H., 2007. Plate tectonic trigger of changes in $p\text{CO}_2$ and climate in the Oxfordian (Late Jurassic): carbon isotope and modeling evidence. *Earth and Planetary Science Letters*, 258: 44–60.
- Mahel, M. & Buday, T. (eds), 1968. *Regional Geology of Czechoslovakia. Part II*. Geological Survey of Czechoslovakia, Praha, 723 pp.
- Marcucci, M. & Prella, M., 1996. The Lumi i Zi (Puke) section of the Kalur cherts: radiolarian assemblages and comparison with other sections in northern Albania. *Ophioliti*, 21: 71–76.
- Marshall, J. D., 1992. Climatic and oceanographic isotopic signals from the carbonate rock record and their preservation. *Geological Magazine*, 129: 143–160.
- Michalík, J., 2007. Sedimentary rock record and microfacies indicators of the latest Triassic to mid-Cretaceous tensional development of the Zliechov Basin (Central Western Carpathians). *Geologica Carpathica*, 58: 443–453.
- Michalík, J., Vašíček, Z. & Borza, V., 1990. Aptychi, tintinnids and stratigraphy of the Jurassic–Cretaceous (Zliechov unit of the Krížna Nappe, Strážovské Vrchy Mts., boundary beds in the Strážovce section Central Western Carpathians, Western Slovakia). *Knihovnička Zemního Plynu a Nafty*, 9a: 69–91. [In Slovak, English summary].
- Mišík, M., 1959. Lithologisches Profil durch die Schichtenfolge des höheren Lias (“Fleckenmergel”) des Gebirges Belanské Tatry. *Geologický Sborník*, 9: 183–187. [In Slovak, German summary].
- Mišík, M., 1999. Contribution to the lithology and petrography of radiolarites in the Western Carpathians. *Mineralia Slovaca*, 31: 491–506. [In Slovak, English summary].
- Mišík, M., Jablonský, J., Ožvoldová, L. & Halásová, E., 1991. Distal turbidites with pyroclastic material in Malmian radiolarites of the Pieniny Klippen Belt (Western Carpathians). *Geologica Carpathica*, 42: 341–360.
- Mišík, M., Sýkora, M., Ožvoldová, L. & Aubrecht, R., 1994. Horná Lysá (Vršatec) – a new variety of the Kysuca Succession in the Pieniny Klippen Belt. *Mineralia Slovaca*, 26: 7–19.
- Mock, R., Sýkora, M., Aubrecht, R., Ožvoldová, L., Kronome, B., Reichwalder, P. & Jablonský, J., 1998. Petrology and stratigraphy of the Meliaticum near the Meliata and Jaklovce villages, Slovakia. *Slovak Geological Magazine*, 4: 223–260.
- Morettini, E., Santantonio, M., Bartolini, A., Cecca, F., Baumgartner, P. O. & Hunziker, J. C., 2002. Carbon isotope stratig-

- raphy and carbonate production during the Early-Middle Jurassic: example from the Umbria-Marche-Sabina Apennines (central Italy). *Palaeogeography, Palaeoclimatology, Palaeoecology*, 184: 251–273.
- Morgans-Bell, H. S., Coe, A. L., Hesselbo, S. P., Jenkyns, H. C., Weedon, G. P., Marshall, J. E. A., Tyson, R. V. & Williams, C. J., 2001. Integrated stratigraphy of the Kimmeridge Clay Formation (Upper Jurassic) based on exposures and boreholes in south Dorset, UK. *Geological Magazine*, 138: 511–539.
- Myczyński, R., 2004. Toarcian, Aalenian and Early Bajocian (Jurassic) ammonite faunas and biostratigraphy in the Pieniny Klippen Belt and the Tatra Mts, West Carpathians. *Studia Geologica Polonica*, 123: 7–131.
- Myczyński, R. & Jach, R., 2009. Cephalopod fauna and stratigraphy of the Adnet type red deposits of the Křížna unit in the Western Tatra Mountains, Poland. *Annales Societatis Geologorum Poloniae*, 79: 27–39.
- Myczyński, R. & Lefeld, J., 2003. Toarcian ammonites (Adnet facies) from the Subtatic succession of the Tatra Mts (Western Carpathians). *Studia Geologica Polonica*, 121: 51–79.
- Navarro, V., Molina, J. M. & Ruiz-Ortiz, P. A., 2009. Filament lumachelle on top of Middle Jurassic oolite limestones: event deposits marking the drowning of a Tethysian carbonate platform (Subbetic, southern Spain). *Facies*, 55: 89–102.
- Nemčok, J., Bezák, Y., Biely, A., Gorek, A., Gross, P., Halouzka, R., Janák, M., Kahan, S., Kotański, Z., Lefeld, J., Mello, J., Reichwalder, P., Rączkowski, W., Roniewicz, P., Ryka, W., Wiczorek, J. & Zelman, J., 1994. *Geologická mapa Tatier (Geological Map of the Tatra Mountains)*, 1: 50 000. Geologický Ústav Dionýza Štúra, Bratislava.
- Nowak, W., 1968. Stomiosphaerids of the Cieszyn Beds (Kimmeridgian – Hauterivian) in the Polish Cieszyn Silesia and their stratigraphical value. *Annales Societatis Geologorum Poloniae*, 38: 275–327. [In Polish, English summary].
- O'Dogherty, L., Carter, E. S., Dumitrica, P., Goričan, Š., De Wever, P., Bandini, A. N., Baumgartner, P. O. & Matsuoka, A., 2009. Catalogue of Mesozoic radiolarian genera. Part 2: Jurassic–Cretaceous. *Geodiversitas*, 31: 271–356.
- O'Dogherty, L., Sandoval, J., Bartolini, A., Bruchez, S., Bill, M. & Guex, J., 2006. Carbon-isotope stratigraphy and ammonite faunal turnover for the Middle Jurassic in the Southern Iberian palaeomargin. *Palaeogeography, Palaeoclimatology, Palaeoecology*, 239: 311–333.
- Ožvoldová, L., 1979. Radiolarian assemblage of radiolarian cherts at Podbiel locality (Slovakia). *Časopis pro Mineralogii a Geologii*, 24: 249–261.
- Ožvoldová, L., 1988. Radiolarian association from radiolarites of the Kysuca Succession of the Klippen Belt in the vicinity of Myjava – Turá Lúka (West Carpathians). *Geologický Zborník – Geologica Carpathica*, 39: 369–392.
- Ožvoldová, L., 1989. Radiolarites from selected localities in the Western part of Klippen Belt. In: Samuel, O. (ed.), *Zborník z paleontologickej konferencie Súčasné problémy a trendy v československej paleontológii*. GÚDŠ, Bratislava. pp. 77–85. [In Slovak, English summary].
- Ožvoldová, L., 1990. Radiolarian microfauna from radiolarites of the Varín part of the West Carpathians Klippen Belt. *Geologický Zborník – Geologica Carpathica*, 41: 295–310.
- Ožvoldová, L., 1992. The discovery of a Callovian radiolarian association in the Upper *Posidonia* Beds of the Pieniny Succession of the Klippen Belt (Western Carpathians). *Geologica Carpathica*, 43: 111–122.
- Ožvoldová, L., 1997. The radiolarian research into Jurassic radiolarite sequences in the Western Carpathians. *Sborník vědeckých prací Vysoké školy báňské – Technické university v Ostravě*, 18–31.
- Ožvoldová, L., 1998. Middle Jurassic radiolarian assemblages from radiolarites of the Silica Nappe (Slovak Karst, Western Carpathians). *Geologica Carpathica*, 49: 289–296.
- Ožvoldová, L. & Frantová, L., 1997. Jurassic radiolarites from the eastern part of the Pieniny Klippen Belt (Western Carpathians). *Geologica Carpathica*, 48: 49–61.
- Ožvoldová, L., Jablonský, J. & Frantová, L., 2000. Upper Jurassic radiolarites of the Czertezik Succession and comparison with the Kysuca Succession in the east-Slovak part of the Pieniny Klippen Belt (western Carpathians, Slovakia). *Geologica Carpathica*, 51: 109–119.
- Padden, M., Weissert, H., Funk, H., Schneider, S. & Gansner, C., 2002. Late Jurassic lithological evolution and carbon-isotope stratigraphy of the western Tethys. *Eclogae Geologicae Helveticae*, 95: 333–346.
- Pearce, C. R., Hesselbo, S. P. & Coe, A. L., 2005. The mid-Oxfordian (Late Jurassic) positive carbon-isotope excursion recognised from fossil wood in the British Isles. *Palaeogeography, Palaeoclimatology, Palaeoecology*, 221: 311–357.
- Pellenard, P., Tramoy, R., Pucéat, E., Huret, E., Martinez, M., Bruneau, L. & Thierry, J., 2014. Carbon cycle and sea-water palaeotemperature evolution at the Middle–Late Jurassic transition, eastern Paris Basin (France). *Marine and Petroleum Geology*, 53: 30–43.
- Pessagno, E. A. & Newport, R. L., 1972. A technique for extracting radiolaria from radiolarian cherts. *Micropaleontology*, 18: 231–234.
- Pisera, A., Satir, M., Gruszczynski, M., Hoffman, A. & Małkowski, K., 1992. Variation in $\delta^{13}\text{C}$ and $\delta^{18}\text{O}$ in Late Jurassic carbonates, Submediterranean Province, Europe. *Annales Societatis Geologorum Poloniae*, 62: 141–147.
- Plašienka, D., 1998. Definition and correlation of tectonic units with a special reference to some Central Western Carpathian examples. *Mineralia Slovaca*, 31: 3–16.
- Plašienka, D., 2012. Jurassic syn-rift and Cretaceous syn-orogenic, coarse-grained deposits related to opening and closure of the Vahic (South Penninic) Ocean in the Western Carpathians – an overview. *Geological Quarterly*, 56: 601–628.
- Plašienka, D., & Ožvoldová, L., 1996. New data about the age of radiolarites from the Belice Unit (Považský Inovec Mts., Central Western Carpathians). *Slovak Geological Magazine*, 1: 21–26.
- Podlaha, O. G., Mutterlose, J. & Veizer, J., 1998. Preservation of $\delta^{18}\text{O}$ and $\delta^{13}\text{C}$ in belemnite rostra from the Jurassic/Early Cretaceous Successions. *American Journal of Science*, 298: 324–347.
- Polák, M. & Ondrejčková, A., 1993. Lithology, microfacies and biostratigraphy of radiolarian limestones, radiolarites in the Křížna nappe of the Western Carpathians. *Mineralia Slovaca*, 25: 391–410.
- Polák, M. & Ondrejčková, A., 1995. Lithostratigraphy of radiolarian limestones and radiolarites of the envelope sequence in the Veľká Fatra Mts. *Slovak Geological Magazine*, 2: 153–158.
- Polák, M., Ondrejčková, A. & Wiczorek, J., 1998. Lithostratigraphy of the Ždiar Formation of the Křížna nappe. *Slovak Geological Magazine*, 4: 35–52.
- Polák, M. & Ožvoldová, L., 2001. Lithostratigraphy of radiolarian limestones and radiolarites of the Hronicum in the Strážovské vrchy Mts. *Slovak Geological Magazine*, 7: 85–89.
- Pszczółkowski, A., 1996. Calpionellid stratigraphy of the Tithonian–Berriasian pelagic limestones in the Tatra Mts (Western Carpathians). *Studia Geologica Polonica*, 109: 103–130.
- Rabowski, F. & Goetel, W., 1925. Les nappes de recouvrement de

- la Tatra. La structure de la zone subtatique. *Sprawozdania Państwowego Instytutu Geologicznego*, 3: 189–224. [In Polish, French summary].
- Rackí, G. & Cordey, F., 2000. Radiolarian palaeoecology and radiolarites: is the present the key to the past? *Earth-Science Reviews*, 52: 83–120.
- Rais, P., Louis-Schmid, B., Bernasconi, S. M. & Weissert, H., 2007. Palaeoceanographic and palaeoclimatic reorganization around the Middle–Late Jurassic transition. *Palaeogeography, Palaeoclimatology, Palaeoecology*, 251: 527–546.
- Rakús, M. & Ožvoldová, L., 1999. On the age of radiolarites from the Manín Unit (Butkov Klippe, Middle Váh valley, Western Carpathians). *Mineralia Slovaca*, 31: 79–86.
- Reháková, D., 2000. Evolution and distribution of the Late Jurassic and Early Cretaceous calcareous dinoflagellates recorded in the Western Carpathian pelagic carbonate facies. *Mineralia Slovaca*, 32: 79–88.
- Reháková, D., 2002. *Chitinoidea* Trejo, 1975 in Middle Tithonian carbonate pelagic sequences of the West Carpathian Tethyan area. *Geologica Carpathica*, 53: 369–379.
- Řehánek, J., 1992. Valuable species of cadosinids and stomiosphaerids for determination of the Jurassic–Cretaceous boundary (vertical distribution, biozonation). *Scripta*, 22: 117–122.
- Rey, J. & Delgado, A., 2002. Carbon and oxygen isotopes: a tool for Jurassic and early Cretaceous pelagic correlation (southern Spain). *Geological Journal*, 37: 337–345.
- Santantonio, M., 1993. Facies associations and evolution of pelagic carbonate platform/basin systems: examples from the Italian Jurassic. *Sedimentology*, 40: 1039–1067.
- Schmid, S. M., Bernoulli, D., Fügenschuh, B., Matenco, L., Scheffer, S., Schuster, R., Tischler, M. & Ustaszewski, K., 2008. The Alpine-Carpathian-Dinaridic orogenic system: correlation and evolution of tectonic units. *Swiss Journal of Geosciences*, 101: 139–183.
- Sucheras-Marx, B., Giraud, F., Pittet, B., Lecuyer, C., Olivero, D. & Mattioli, E., 2013. Duration of the Early Bajocian and the associated $\delta^{13}\text{C}$ positive excursion based on cyclostratigraphy. *Journal of the Geological Society*, 170: 107–118.
- Sujkowski, Z., 1932. Radiolarites des Karpates Polonaises Orientales et sur leur comparaison avec les radiolarites de la Tatra. *Sprawozdania Państwowego Instytutu Geologicznego*, 7: 97–168. [In Polish, French summary].
- Suzuki, H., Wegerer, E. & Gawlick, H. J., 2001. Zur Radiolarienstratigraphie im unteren Callovium in den Nördlichen Kalkalpen – das Klauskogelbachprofil westlich von Hallstatt (Österreich). *Zentralblatt für Geologie und Paläontologie*, 2000: 167–184.
- Sýkora, M. & Ožvoldová, L., 1996. Lithoclasts of Middle Jurassic radiolarites in debris flow sediments from Silica Nappe (locality Bleskový Prameň, Slovak Karst, Western Carpathians). *Mineralia Slovaca*, 28: 21–25.
- Vörös, A., 2012. Episodic sedimentation on a peri-Tethyan ridge through the Middle-Late Jurassic transition (Villány Mountains, southern Hungary). *Facies*, 58: 415–443.
- Weissert, H. & Erba, E., 2004. Volcanism, CO₂ and palaeoclimate: a Late Jurassic–Early Cretaceous carbon and oxygen isotope record. *Journal of the Geological Society*, 161: 695–702.
- Weissert, H. & Mohr, H., 1996. Late Jurassic climate and its impact on carbon cycling. *Palaeogeography, Palaeoclimatology, Palaeoecology*, 122: 27–43.
- Widz, D., 1991. Upper Jurassic radiolarians from radiolarites of the Pieniny Klippen Belt (Western Carpathians, Poland). *Revue de Micropaléontologie*, 34: 231–260.
- Wieczorek, J., 1990. Main phases of the geological evolution of the western Tethys – an outline. *Kwartalnik Geologiczny*, 33: 401–412. [In Polish, English summary].
- Wieczorek, J., 2001. Condensed horizons as turning events in passive margin evolution: the Tatra Mts examples. *Zentralblatt für Geologie und Paläontologie, Teil 1*, 2000: 199–209.
- Wierzbowski, A., 1994. Late Middle Jurassic to earliest Cretaceous stratigraphy and microfacies of the Czorsztyn Succession in the Spisz area, Pieniny Klippen Belt, Poland. *Acta Geologica Polonica*, 44: 223–249.
- Wierzbowski, A., Jaworska, M. & Krobicki, M., 1999. Jurassic (Upper Bajocian–lowest Oxfordian) ammonitico-rosso facies in the Pieniny Klippen Belt, Carpathians, Poland: its fauna, age, microfacies and sedimentary environment. *Studia Geologica Polonica*, 115: 7–74.
- Wierzbowski, H., 2002. Detailed oxygen and carbon isotope stratigraphy of the Oxfordian in Central Poland. *Geologische Rundschau*, 91: 304–314.
- Wierzbowski, H., 2004. Carbon and oxygen isotope composition of Oxfordian–Early Kimmeridgian belemnite rostra: palaeoenvironmental implications for Late Jurassic seas. *Palaeogeography, Palaeoclimatology, Palaeoecology*, 203: 153–168.
- Wierzbowski, H., Dembiczyk, K. & Praszker, T., 2009. Oxygen and carbon isotope composition of Callovian–Lower Oxfordian (Middle–Upper Jurassic) belemnite rostra from central Poland: A record of a Late Callovian global sea-level rise? *Palaeogeography, Palaeoclimatology, Palaeoecology*, 283: 182–194.
- Zempolich, W. G. & Erba, E., 1999. Sedimentologic and chemostratigraphic recognition of third-order sequences in resedimented carbonate: the Middle Jurassic Vajont Limestone, Venetian Alps, Italy. In: Harris, P. M., Saller, A. H. & Simo, J. A. (eds), *Advances in Carbonate Sequence Stratigraphy: Applications to Reservoirs, Outcrops and Models*, Society of Economic Paleontologists and Mineralogists, Special Publication, 63: 335–370.